An *in vivo* analysis of the immune response to a malaria vaccine

The role of the chemokine receptor CXCR3 in the innate and adaptive immune response after genetically attenuated *Plasmodium* immunization

MASTER THESIS

In partial fulfillment of the requirements for the degree

"Master of Science in Engineering"

Master program:

"Biotechnology"

Management Center Innsbruck

Supervisor

Seattle Biomedical Research Center

Stefan Kappe, Ph.D.

Internal supervisor:

Mag. Carmen Nußbaumer, Ph.D.

Author:

Lisa Wegmair, BSc.

1610352024

Declaration of academic integrity

I hereby confirm that the present master thesis on is solely my own work and that if any text passages or diagrams from books, papers, the Web or other sources have been copied or in any other way used, all have been acknowledged and fully cited.

The thesis has not been shown before to examiners in a similar way nor has it been published yet.

Eidesstattliche Erklärung

„Ich erkläre hiermit an Eides statt, dass ich die vorliegende Masterarbeit selbständig angefertigt habe. Die aus fremden Quellen direkt oder indirekt übernommenen Gedanken sind als solche kenntlich gemacht.

Die Arbeit wurde bisher weder in gleicher noch in ähnlicher Form einer anderen Prüfungsbehörde vorgelegt und auch noch nicht veröffentlicht.“

Seattle, 25.09.2018

Acknowledgment

I wish to express my sincere thanks to my PI Stefan Kappe, my supervisors Nana Minkah and Brandon Sack for providing me with the necessary trainings and facilities for conducting all experiments necessary for writing my master thesis. It has been a very difficult project with many obstacles that required a lot of effort and time, but with the help of them and the strong support of my family and friends, it was possible to create a master thesis that is the foundation of a new future project.

I am absolutely proud of having been given the opportunity to be a part of that incredible team of international researchers which put all their energy and knowledge together to understand and cure malaria.

Abstract

Malaria is a severe parasitic disease caused by *Plasmodium* parasites and leads to half a million deaths worldwide each year. No malaria vaccine exists, and current preventive measures and anti-malaria drugs have been unable to limit malaria-associated disease and death. Therefore, there is a tremendous need to develop an effective malaria vaccine.

One approach is to target the pre-erythrocytic liver-stage where the parasite load is low, and the patient remains devoid of clinical symptoms. Of the pre-erythrocytic vaccine methods, immunization with whole parasites where parasite development within the liver is arrested, has become especially attractive. These genetically attenuated parasite (GAP) vaccines mediate protection against a wildtype *Plasmodium* infection mainly through natural killer T (NKT) cells and cytotoxic (CD8+) T cells. However, the mechanisms that are involved in the establishment of a protective immune response after GAP vaccination are not fully understood, especially the recruitment and maintenance of the effector (memory) cells into the liver. Therefore once there is a better understanding of these processes, it might be possible to enhance the efficacy of GAP vaccines.

Cytokines and chemokines generally mediate the recruitment and maintenance of immune cells to the inflamed tissue. An analysis of the liver transcriptome after GAP infection showed that the chemokines CXCL9 and CXCL10 are highly upregulated and further their receptor, CXCR3, is abundant on the protective memory CD8+ T cells and NKT cells.

Therefore the approach for this master thesis was to find out if the chemokine receptor CXCR3 were involved in the immune response after GAP vaccination. This was investigated through an *in vivo* imaging system (IVIS) analysis and a newly developed multicolor flow analysis by using CXCR3 knockout mice and C57BL/6J mice that were treated with a cell-depleting antibody, binding specifically to CXCR3.

Treatment with a CXCR3 antibody significantly reduced the protection induced by the GAP vaccine, but the loss of CXCR3 in the knockout mice had surprisingly no impact on either innate or adaptive immune control. However, it was observed that the loss of CXCR3 limits the recruitment of the immune CD8+ T cells into the livers of immunized mice at an early stage of immunization.
As such, it can be proposed that CXCR3 are essential for the early recruitment into the liver, but it has no impact on protection after immunization.

Kurzfassung

Malaria gilt als eine der häufigsten verbreiteten Infektionskrankheiten in den Subtropen, wodurch es jährlich knapp eine halbe Millionen Todesfälle gibt. Der Erreger sind verschiedene Arten von *Plasmodium,* welche von den weiblichen *Anopheles* Mücken übertragen werden.

Eine beständige Impfung gegen Malaria gibt es bisher noch nicht, aber eine vielversprechende Innovation sind die „ganzen Parasiten“ Vakzine (gentechnisch abgeschwächte Parasiten- GAPs). Diese bringen den Vorteil, dass sie bereits im nicht symptomatischen Leber Stadium von Malaria wirksam werden, wo die Anzahl der Parasiten, im Vergleich zu dem darauffolgenden symptomatischen Blutstadium, noch gering ist. Es wurde bereits veröffentlicht, dass diese in *in Vivo* Studien eine schützende Wirkung gegen darauffolgende wildtyp Infektionen zeigen. Zytotoxische T Zellen (CD8+) und natürliche Killer T Zellen (NKT) sind die Haupteffektor Zellen in diesem Prozess.

Die fundamentalen Mechanismen und involvierten Schlüsselmoleküle in der Immunantwort nach den Immunisierungen sind weitreichend noch nicht erforscht. Zentral stellt sich die Frage, wie diese schützenden Zellen in die Leber rekrutiert und zurückgehalten werden. Das würde die Herstellung eines effektiven Vakzines einen Schritt weiter bringen, um eine verstärkte Immunreaktion gegen eine nachfolgende wildtyp Infektion hervorzurufen.

Bei vielen Infektionskrankheiten spielen pro-inflammatorische Chemokine eine tragende Rolle im Rekrutierungsprozess und der Zurückhaltung von Immune Zellen in entzündeten Geweben. Der Chemokin Rezeptor CXCR3 wird von den CD8+ und NKT Zellen exprimiert und auch die Liganden CXCL9 und CXCL10 sind dominant präsent in der Leber nachdem GAP verabreicht wurde. Demnach ist es unabdingbar, den Chemokin Rezeptor und seine Liganden näher zu betrachten.

Daher beschäftigte sich diese Arbeit mit der Frage, ob der CXCR3 Rezeptor mit seinen Liganden CXCL9 and CXCL10 in die Immunantwort nach GAP Injektionen eine Rolle spielt. Das wurde mittels *in vivo* Imaging System und Multicolor Durchflusszytometrie Analysen ermittelt, indem CXCR3 knockout Mäuse und C57BL/6J Mäuse (mit Zellen eliminierenden CXCR3 Antikörper Behandlung), verwendet wurden.

Es zeigte sich das der Schutz gegen eine wildtyp Infektion verloren geht, nachdem die CXCR3 exprimierenden Zellen mittels einem CXCR3 Antikörper eliminiert wurden, Wohingegen der Verlust des CXCR3 Rezeptors in knockout Mäusen hatte keinen Einfluss auf die schützende angeborene und erworbene Immunantwort. Jedoch wurde

festgestellt, dass in den CXCR3 Knockout Mäusen weniger CD8+T Zellen in die Leber der immunisierten knockout Mäuse rekrutiert wurden am Anfang einer Immunisierung.

Table of Contents

1 Introduction

Malaria is one of the most severe parasitic diseases. It is caused by *Plasmodium* species and affects approximately 40% of the world's population and caused an estimated 445 000 deaths worldwide in 2016. The highest risk is faced mainly in the subtropical regions of Africa, South America and Asia. [1] Emerging drug resistance to conventional antimalarial drugs like chloroquine, and the lack of new anti-malarials have significantly contributed to the inability to eradicate Malaria. However, the development of new anti-malarials has been slowed down by the vast size of the *Plasmodium* genome and the complexity of the *Plasmodium* life cycle. The parasite goes through insect and animal hosts and develops multiple different developmental stages. In vertebrates, the sporozoites (infectious stage of *Plasmodium*) progress from the skin into the liver (pre-erythrocytic stage) and go further into blood stages (erythrocytic stage), which cause the characteristic symptoms of malaria and similarity to the infected eukaryotic host.

Therefore there is a tremendous demand to develop new treatments for the people located in endemic areas, for infected patients and people traveling to affected areas. A promising vaccine strategy are genetically-attenuated *Plasmodium* parasites (GAPs), in which liver development is stopped by removal of critical genes and cannot go further into the blood stage.[2] After multiple administrations of GAP into mice, they are able to control a following wildtype *Plasmodium* infection. [3,4] This establishes an extraordinary opportunity to carefully examine the asymptomatic state of malaria, and more importantly it can be seen as a potential vaccine for immunization. However, the fundamental mechanism and key players in the process of creating an immune response specifically against GAP sporozoites are poorly understood and need more investigation to be able to design an advanced vaccine platform.

It is known that under inflammatory conditions (injury, cell death and infections) cell signaling leads to the production of cytokines and chemokines creating a gradient that results in the recruitment of immune cells expressing cognate receptors.

The chemokines CXCL9 and CXCL10 play an important role in recruiting lymphocytes into inflamed tissues like brain, kidney, pancreas, spleen, liver [5–8]. They also have an influence on T cell generation [9] and retention of immune cells to stay in the inflamed tissue. [8]

During GAP infection, RNAseq data suggests that CXCL9 and CXCL10 are among the top 1% of upregulated genes in the parenchymal cells of the liver, such as hepatocytes (Appendix 1) and liver sinusoidal endothelial cells (LSECs) (Appendix 2). Moreover, the receptor CXCR3 of the chemokines CXCL9 and CXCL10 is expressed on the immune cells, like natural killer T cells and memory cytotoxic T cells, [10,11] which are described to be crucial for protection against wildtype sporozoites after GAP immunization.

The relevance of the study of the CXCR3 and its chemokines is biologically relevant and contributes novel insights into the innate and adaptive immune response to pre-erythrocytic GAP immunization. In case they show a significant impact they will contribute to develop an effective vaccine.

2 Theory and Background

Malaria is an infectious disease caused by certain *Plasmodium* species, mostly *P. falciparum, P. ovale, P. malariae, P. knowlesi* and *P.vivax* for humans and *P.yoelii* and *P.berghei* for rodents which show unique characteristics in its own and have to be evaluated separately. However, *P. yoelii* is an important animal model for studying human malaria *in vivo* in mice, especially in parasite-host interactions and liver stage assessments, due to similarities to conserved gene profiles to *P.falciparum* and significant better characteristics in the early immune response during liver stages in comparison to *P.berghei.* [12–14]

2.1 Malaria life cycle

Malaria has a characteristically complex life cycle (Figure 1). *Plasmodium* sporozoites are transmitted by female *Anopheles* mosquitos to the hosts where they undergo certain genetic and phenotypic changes to spread in their host's systems. A bite of the mosquito releases approximately 100 sporozoites [15] out of the salivary glands into the host's dermis and glide within the first few hours into the blood vessels.[16] The parasites in the blood stream enter the liver through the portal vein and arrive in the liver sinusoids, which are tight vascular channels that supply the liver tissue. Here the parasites traverse tissue cells including epithelial cells, sinusoidal endothelial cells, hepatic stellate cells and also overcome immune cells like phagocytic Kupfer cells and dendritic cells [17] to invade one of the millions of hepatocytes in the liver tissue (Figure 2).

The exact mechanism and key proteins involved in traversal and invasion are still under investigation. However, the surface protein CSP (circumsporozoite protein) and the secreted microneme protein TRAP (Thrombospondin-Related Anonymous Protein) seem to have a crucial role in the process of invasion. [18,19] This process can elicit an inflammation response through the wounded traversed and invaded cells. [17]

After the successful invasion into the hepatocytes (main cell in parenchymal tissue of the liver) and form a parasitophorous vacuole which originates from the host and thereby protects the parasite from the immune system. [20,21] The parasite develops into approximately 50 000 merozoites within 48h to 54h (for *rodent Plasmodium)* and 7-10 days (for human *Plasmodium)* [22], which are released into the bloodstream again and infect red blood cells (lethal strains) or just reticulocytes (which are non-matured red blood cells (non-lethal strains, like *P. yoelii*).

In the next step merozoites develop into trophozoites and once they reached the schizont stage, they rupture the cell and differentiate into the asexual state or transform into gametocytes for the sexual stage while undergoing many genetic changes. This is the stage where malaria shows its characteristic symptoms, like fever and chills, severe anemia, metabolic acidosis and respiratory distress [23]. If a mosquito takes a blood meal, the gametocytes go into the midgut of the insect and the micro- (male) and macro-gametocytes (female) fuse to a zygote to an ookinete and develop into a sporozoite. After two weeks the sporozoites travel to the salivary glands of the mosquito and during the next blood meal they are re-released into the bloodstream of the host (Figure 1). [18,24]

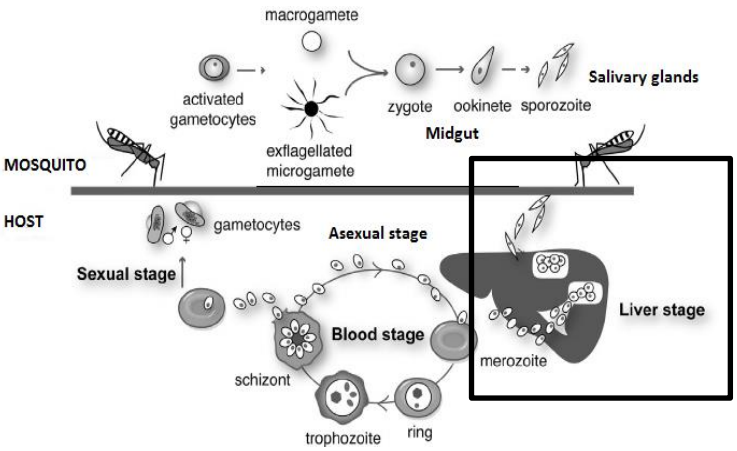

Figure 1: Life cycle malaria parasite [25]

The mosquito releases the sporozoites out of the salivary glands into the dermis of the host and they migrate into the liver (black framed window). The sporozoites develop further into merozoites and are released into the blood stream again where they infect red blood cells and undergo the maturation from ring stages into schizonts. The cell raptures and releases them where they go into asexual replication in new infected red blood cells or differentiate into gametocytes (sexual stage). Once the mosquito takes a blood meal again the gametocytes are activated in the gut of the insect where the female macrogametes and the male microgametes fuse to a zygote and develop further into sporozoites. They travel to the mosquitos salivary glands and can be injected again into a host.

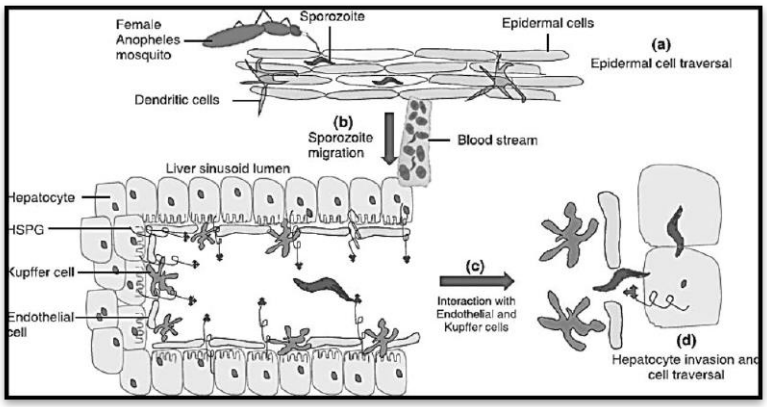

Figure 2 Schematic representation of sporozoites traversal and invasion into the liver [26]

Black framed window of figure1 is a more detailed illustration of the sporozoites entering the host and invading into the hepatocytes, that causes the pre-erythrocytic stage of Malaria. a) The injected sporozoites in the skin undergoing epidermal cell traversal to go into the blood stream. b) Arrival in the liver sinusoids c) Traversing epithelial cells and immune cells to invade the hepatocytes for further replication

2.2 Liver pre-erythrocytic stages

The pre-erythrocytic stages were thought to not provoke a significant immune response due to multiple reasons. First of all the patient shows no clinical phenotype during liver infection, the second reason is that there is just a very low parasite burden at the beginning of the infection that seemed to be negligible in comparison to the enormous amount of parasites during blood stage infection. Thirdly, the liver is known to be an organ with an attenuated immune reaction because of the constant exposure to antigens coming mainly out of the gut [27], and finally it was not possible to stop the parasites in the liver stage, so it was very challenging to find the right time point to distinguish between liver and blood stage clearly.

The promising discovery of genetically-attenuated plasmodium parasites (GAP), which stop in different developmental stages of the liver and do not progress to exoerythrocytic merozoites [2], It establishes an extraordinary opportunity to target pre-erythrocytic stages of *Plasmodium* and create a vaccine due to protective immune response to the following wildtype infection, which is already eliminated at the beginning of the infection before the *Plasmodium* reaches high numbers and go into the symptomatic blood stage. [3,4]

Whole sporozoite vaccines

There are two main approaches for targeting pre-erythrocytic liver stages in the malaria vaccine development. On the one hand the subunit vaccines, on the other hand, the whole sporozoite immunization.

The efficacy of the whole live-attenuated sporozoite immunization have so far been unmatched by any subunit malaria vaccines in development, including the most advanced CSP-based RTS, S vaccine candidate currently being tested in phase 3 clinical studies, which showed just 30–50% protective efficacy and a relatively short duration of protection because of the vaccine epitope that targets a not highly conserved central repeats and the C-terminal of *P. falciparum* CSP protein. [28, 29]

Therefore the whole sporozoite vaccines are promising approaches to overcome the main problems of subunit vaccines. They can be differentiated between the non-replicating radiated attenuated sporozoites (RAS), chemoprophylaxis treatment with a combination of wildtype sporozoites administration (CPS), known as infection-treatment immunization (ITI) [30] and the non-replicating and replicating genetically attenuated *Plasmodium* (GAP). [3]

CPS is the administration of wildtype sporozoites with subsequent treatment of chloroquine to avoid the establishment of an infectious blood stage. The safety aspect of this treatment is critical even though the protection against the following infection is efficient. [31]

The gold standard of whole sporozoite vaccine candidates are radiated attenuated sporozoites (RAS) that lost the ability of replication and stop in the early stage of the liver with variations in the generated generations and show protection against a wildtype infection after several RAS immunization in mice and human (vaccine PfSPZ). [32], Most studies have been done on RAS sporozoites because they have been designed in the last century and many studies in rodents, primates and humans have been conducted. [33–35]

However, the most promising candidate of the whole sporozoites, seemed to be GAP because they are genetically defined in comparison to RAS and show enhanced immunogenicity and efficacy while maintaining safety. Many fundamental mechanisms can be learned out of RAS studies, but if these apply for GAP as well, have to be investigated separately.

Therefore in this work, the focus remains exclusively on the most recently invented GAPs which stop in different developmental stages of the liver and do not progress to exoerythrocytic merozoites. [2] The sporozoites in the liver stop whether in an early stage without any biomass expansion (Early Arresting GAP) or a later replicative liver stage (Late Arresting GAP), depending on the mutated genes.

In the experiments, a late arresting GP is used and consists of are knockout FabB/F$^{/-}$ *P.yoelii* sporozoites which have been created by using a homologous cross-over recombination strategy. [36] FabB/F is a critical enzyme in type 2 *de-novo* fatty acid synthesis pathway which is involved in the development of the sporozoites' apicoplast (coating plastid organelle) is inhibited that no establishment of a blood stage is possible. [37]

The expression of many pre-erythrocytic and erythrocytic proteins on the outer surface (e.g., CSP, TRAP, and many others) [18] is given due to the later liver stage. Therefore they contribute to broad antigen stimulation and allows to achieve partly or sterile control against *Py* (*Plasmodium yoelii*) WT sporozoites in C57Bl/6J mice after multiple GAP sporozoite immunization. [4,38,39]

2.3 Immune responses to pre-erythrocytic malaria

Recent findings have shown that pre-erythrocytic stages induce a pronounced innate and later on an adaptive immune response which is described in the next two chapters.

2.3.1 Innate immune response

Although the immune response to the non-symptomatic *Plasmodium* infection in the liver was not to be sensed to be previously, it has been shown that after the sporozoites entering the liver and hepatocytes, the immune response is visible.

Using RNA sequencing, it has been shown that rodent malaria liver-stage infection stimulates a robust innate immune response including type I interferon (IFNα/IFNβ) that is induced by IRF3 (interferon regulatory factor) [40] and IFNγ pathways (Figure 3). [10, 41]

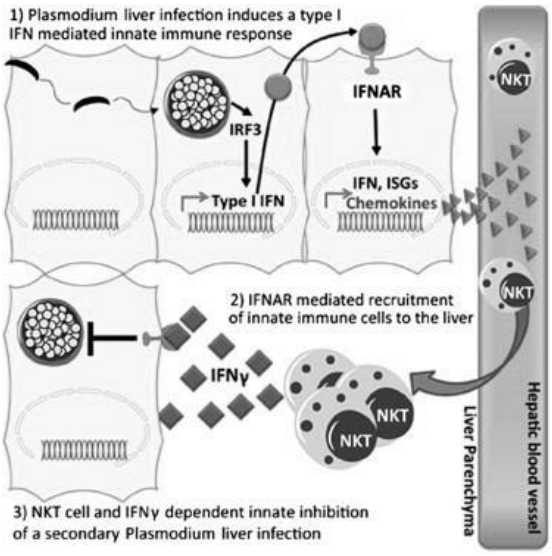

Figure 3: Innate immune response to *Plasmodium* infection in hepatocytes

The invasion of sporozoites into the hepatocytes results in the activation of Type1 IFN expression that is mediated by IRF3. IFN1 is released and binds to its receptor IFNAR. This induces a signaling cascade for the expression of interferon-stimulated genes (e.g., chemokine expression and more IFN1): The chemokines recruit innate immune cells (NKT cells) to the inflammation site: They can control the infection which is dependent on IFNγ.

The induced type I Interferon binds to the IFNAR receptor and leads to the induction of the interferon-stimulated genes (ISG), such as pro-inflammatory chemokines. In particular, CXCL9 and CXCL10 are ISGs and are highly upregulated during FabB/F infection in hepatocytes (Appendix 1) and LSECs (Appendix 2) recruit more lymphocytes out of the blood into the infected liver. [42]

It is known that the C57BL/6 mice emerge a robust innate immune response after 3 days post FabB/F sporozoite administration. After 3 days (72h) post FabB/F infection the present cells were natural killer cells (NK, NKT, CD4+, CD8+ and other immune cells) [10], The NK and NKT cells belong to the innate immune response, however the transmission to the adaptive immune response (activation of CD4+T cells and CD8+T cells) overlap at a certain point with the innate immune response.
A subgroup of NKT cells, the CD1d restricted NKT cells (TCR receptor binds to CD1d molecule which is activated through its antigen α-Galactosylceramide [43]) are dependent from IFN1 and IFNγ signaling and seem to be crucial for controlling liver burden that is tested in several knockout mice, whereas the other cell types did not alter the protection pattern. [10]

So the assumption is that IFN-1 induction results in elevated CXCL9 and CXCL10 production by hepatocytes and LSECs. There is a 14,1 fold change in transcription level for CXCL9 and a 17 fold change for CXCL10 in comparison to uninfected mice. [10] As a result the cytokines might recruit CXCR3 (receptor of CXCL9/CXCL10)-expressing cells, like CD4+, CD8+, NK, NKT and plasmacytoid dendritic cells (pDc) to the inflamed tissue. [42] Some cells are involved in controlling the liver infection, like NKT cells and CD8+ cells and others are responsible for enhancing the immune response through producing signaling molecules and decoy more immune cells. [44, 45]

2.3.2 Adaptive immune response

The adaptive immune response, also known as acquired immune response is developing after the immediately responding innate immune response (Figure 4). It is in contrast to the innate response highly specific against the pathogen and consists of humoral and cytotoxic mechanisms which are mediated through B and T lymphocytes (CD4+ and CD8+).

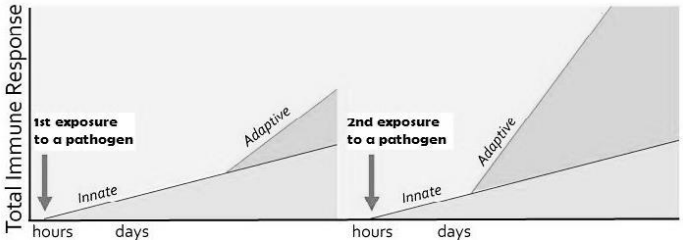

Figure 4: Innate and adaptive immune response over time after the first and second exposure to a pathogen [46]

Left: The first time of exposure to a pathogen the innate immune response leads to an adaptive immune response after several days

Right: The secondary exposure to the same pathogen creates an enhanced and faster adaptive immune response than at the first time

After GAP immunization the influence of the innate immune response to the adaptive immune response to establish protecting cell populations is hardly understood and needs further investigation.

In general, the link of the innate to the adaptive immune response is antigen presenting cells (APC). In the liver APCs are mainly different types of dendritic cells, Kupfer cells, infected cells e.g. hepatocytes and liver sinusoidal endothelial cells (LSECs) that mediate the activation of naïve T cells in the lymphoid tissues through the presentation of *Plasmodium*-specific antigens (especially CSP) [47] on the major histocompatibility complexes I and II (MHC complex). In case of CD8+ T cell activation in liver stage, they recognize MHC I complexes. [48] Generally, the antigen presentation in the liver seems to be weak because of the constant exposure to external antigens from the gut. However, lipid-rich DCs produce inflammatory cytokines and have immune stimulatory properties in the liver. [49]

Furthermore, LSEC cross-present antigens released from hepatocytes [50] to naıve CD8+ T cells without inflammation to reach functional maturation [51] and differentiate into memory cells [52]. Such LSEC-induced generation of memory T cells may occur when pathogens escape innate immunity through preventing cross-priming by DCs that requires an inflamed environment. [53]

Depending on the type of the naïve T cell precursor, the activated T cell has whether CD8+ cytotoxic properties (kill *P. yoelii* infected cells by the release of effector molecules, like granzyme, perforin, IFNγ [54] or differentiate into CD4+ T helper cells. The CD4+ cells enhance the immune response through pro-inflammatory cytokine production that recruits more immune cells to the inflamed tissue, regulate the humoral response, and have other regulatory functions. The general activation marker CD44 helps to distinguish between antigen-experienced and naïve T cells.[55]

After the peak of the adaptive immune response, the majority of responding T cells die and 5 to 10% survive to become memory T cells, which show a dormant state and are circulating or residential in lymphoid and non-lymphoid tissues. They can be reactivated very quickly after a second infection of the same pathogen. However, the adaptive response is more enhanced than in the first time (Figure 4). [56] The immune system is getting educated with a subunit of a pathogen or with a less potent attenuated parasite, which allows controlling a secondary infection. Vaccination is based on these principles.

Findings show that the recently discovered CD8+ tissue resident memory **(Trm)** cells [57] play a crucial role in protection against pre-erythrocytic malaria infection by using the whole sporozoites vaccine of non-replicating RAS sporozoite vaccines.[58] However, before the Trm were discovered, the protection properties of memory CD8+ cells are proposed even for GAP sporozoite. [11] Therefore it might be possible that Trm cells are also essential after GAP immunization for protection, but still has not been published.

Moreover, the successful establishment of a larger residential CD8+ memory population in the liver after primary infection is highly dependent on CD4+ support. [59] The resident CD8+ memory T cells form likely clusters with CD4+ cells and antigen presenting cells, to be supported in their retention in the tissue and reactivation after an infection, stimulated by constant secretion of small amounts of chemokines and pro-inflammatory molecules [60] and up-regulation of certain surface markers for a lifetime (CD69, CXCR6, CXCR3). [61, 62]

The Trm cells are patrolling in the sinusoids while crawling on the vascular epithelial surfaces to surveillance the organ. [58] They do not show any migration to the second organism in parabiosis studies [63] that implies that they are truly tissue resident and don't leave into the periphery. After a *Plasmodium* infection the LFA1-ICAM-1 (intercellular adhesion molecule 1) interaction and allows the cells to be recruited to the liver immediately. [64] In general Trms are tissue dependent (skin, lung, gut, liver, spleen) and show differences in each of them and therefore also the immune response to pathogens differs. Therefore it should be pointed out that for instance CD103 is not required for retention in the liver like in other tissues (skin, spleen, lymph nodes) whereas ICAM1 seems to be required for liver and lung Trm cell retention. [64, 58]

Analyzing the protective CD8+ liver tissue resident T cells is difficult because the population size is very small and they need a precise distinction from other memory cell populations, like central memory T (Tcm) cells (recirculating in blood and secondary lymphoid tissues) and effector memory T (Tem) cells (circulating in blood and non-lymphoid tissue). [65] Homing markers help to differentiate between them. The lymph node homing receptor CD62L is present on Tcm cells, but is not expressed by Trm cells, whereas the constant expressed early activation marker CD69 and the chemokine receptors CXCR6 and CXCR3 [58, 66] are present on Trms (not on Tem cells).

2.3.3 Chemokines CXCL9, CXCL10, CXCL11 and their receptor CXCR3

Under inflammatory conditions, cell signaling leads to the production of cytokines and chemokines create a gradient that results in the recruitment of immune cells expressing cognate receptors. The response to inflammation is regulated in the patient through complex interactions between cytokines and chemokines that provide crucial communication signals resulting in the effective development of innate and adaptive immune response. Cytokines are small pro-inflammatory proteins (around 10kDa) activated through primary inflammatory cytokines like IFNγ, IFN1, TNF that are secreted by for example macrophages (Kupfer cells in the liver) or inflamed tissue cells, like hepatocytes and liver sinusoidal endothelial cells (LSECs) in the liver. They distinguish from general primary attractants through their ability to attract only specific lymphocytes (mainly activated T cells, regulatory T cells, macrophages, neutrophils) to the inflamed tissue to generate an individual designed response to specific pathogens.

The chemokine ligands can be distinguished through their structure and function. Structurally the CXC chemokines possess one amino acid in between their first two cysteine residues [67] and bind via their C-terminal α-helix to a glycosaminoglycan (GAGs) on the surface of endothelial cells to form an immobilized chemotactic gradient, which guides passing immune cells towards the source of chemokine secretion. [68, 69] In the case of the pro-inflammatory chemokines CXCL9, CXCL10 and CXCL11 guiding T cells, [70] especially Th1, CD8+ and NK (T) cells to the inflamed tissue through their CXCR3 receptor. [70]

The induction of CXCL9, 10 and 11 is mediated through the molecules IFNγ, IFNα and IFNβ and TNFα. CXCL11 is only activated through IFNβ and IFNγ together, whereas CXCL9 is expressed from cells in the inflamed tissue cells after IFNγ influence and CXCL10 is induced through an IFN1 response (IFNα, IFNβ). However, it is possible to induce the IFN response and further on the chemokines through many different pathways, for example, it can be initiated by innate sensors, such as the toll-like receptor and RIG-I, as well as through IFN-regulatory factor 3 [71], which makes that system even more complex to understand.

Moreover, the chemokines show slightly different affinities to their receptor, CXCL11 shows the highest affinity to the receptor followed by CXCL10 and CXCL9 that implies that they create a highly complex system of lymphocyte attraction and other cellular mechanisms. [72]

The chemokine system shows contradictions in the question if the ligands are redundant in their expression. In case it is true, it would imply that the distribution of the chemokines are dependent on each other and can fulfill the same functions in case one is not upregulated after infection. However, there are others who propose that the ligands for CXCR3 induce different effects, that CXCL9 and CXCL10 show inflammatory effects while CXCL11 has been shown to induce the development of T_{regs}, and thus is an anti-inflammatory response in auto-inflammatory diseases. [73] Thus, the complexity of the chemokine system and the contradictory consensus in different infections, the system must be evaluated in each case separately.

In most cases, the pro-inflammatory receptors possess more than two ligands, like the CXCR3 receptor that has three ligands. [74] Besides this chemokine system, 20 more receptors are known and 50 additional chemokines, which possess homeostatic and inflammatory properties. [75] In particular, the pro-inflammatory chemokines CXCL9, CXCL10 and CXCL11 bind to different regions of a seven transmembrane CXCR3 receptor and induces a G-protein mediated response. The subunits of the receptor change their confirmation after a chemokine ligand binds. This allows the bound GDP to exchange with GTP that separated the α-subunit from the β-γ-subunit and both can induce a specific downstream response. [76]

The CXCR3 receptor can be found on CD8+ cells, CD4+ (mainly T_{H1} cells, T_{H2} cells, T_{17}, T_{regs}), NKT cells and some epithelial cells and even on the IFN producing plasmacytoid dendritic cells and a subset of B cells in the blood [42, 75] In particular, after activation the CD8+ T cells and CD4+ T cells show a high CXCR3 expression and certain subsets of CD8 T memory subsets. [77, 58] In some instances some receptors are continuously expressed to be involved in recruiting, establishing or maintaining cell population in tissues.

3 Material and Methods

3.1 Mice

The mice that were used in the experiments and flow panel development were inbred C57BL/6J and purchased from Jackson Laboratory (Strain no.000664).

Genetics C57BL/6J

In the case of the used mouse strain in the experiments (C57BL7/6J) they only express CXCL9 and CXCL10, whereas not CXCL11, due to a single base deletion in the reading frame of the CXCL11 gene that makes it easier to evaluate the system in these mice. [42]

The mice that were used for sporozoite production (described in 3.2.1) were outbreed Swiss Webster mouse (ENVIGO, Hsd.ND4).

Knockout mice:

For the experiments using CXCR3 knockout mice, mice were obtained from Jackson Laboratory; B6.129P2-Cxcr3/J, 005796 and then bred in the vivarium at the Center for Infectious Disease Research. They had the C57BL/6 genetic background and the CXCR3 gene was knocked out through a targeted mutation and replaced by a bacterial lacZ, β-galactosidase expression cassette.

3.1.1 Ethical statement

All murine studies have been performed according to the regulations of the institutional animal care and use committee. Approval was obtained from the Seattle BioMed Experimental Animal Ethical Committee.

3.1.2 Injections and blood collection

The injections were whether intraperitoneally into the lower end of the abdominal (Ketamine, antibodies, infected blood) or intravenously through retro-orbital injections (sporozoite immunization).

Blood samples are obtained via retro-orbital bleed (for serum extraction), cardiac puncture (terminal procedure), tail tip bleed or from a frozen stock.

3.1.3 Anesthesia and Euthanasia

Anesthesia:

A Ketamine solution containing 5ml of Ketamine (100 mg/ml) and 500 µl of Xylazine (100 mg/ml) and 34.5ml of sterile PBS was used to anesthetize the mice. Ketamine is under drug supervision law and therefore is protocolled each time of usage.

Isoflurane mixed with O_2 in the gas chamber is used to anesthetize the mice before they were injected i.v. via retro-orbital injection and for anesthetizing them for IVIS analysis.

Euthanasia:

A terminal procedure is to kill the mice with CO_2 for 5min and additionally, a cervical dislocation has to be done to ensure the death of the animal.

3.1.4 Breeding

A breeding cage contained two females and one male mouse. After three weeks of pregnancy the female gave birth and is separated from the male. An average litter contained five to ten pups and the weaning date was18 days after the date of birth, where the pups are transferred to cages where males and females are separated. After 8 weeks in total, the mice were ready to be used in experiments.

3.2 *Plasmodium yoelii* life cycles in mice and mosquitos for sporozoite production

3.2.1 *P. yoelii* FabB/F sporozoite production in *Anopheles stephensi* mosquitos

One life cycle took 24-28 days until the sporozoites could be dissected out of the mosquito's salivary glands.

On day zero, 200 µL of frozen infected blood was thawed and injected intraperitoneally (i.p.) into an outbreed Swiss Webster mouse (ENVIGO, Hsd.ND4). On day six 1- 2% of parasitemia (infected red blood cells) were counted on a thin blood smear on a slide made out of a drop of blood from the mouse's tail tip. If the parasitemia was high enough, the next day a cardiac puncture of the mouse (getting approximately 1ml blood) was performed and the blood diluted with PBS to 1% parasitemia. 150 µL was then injected i.p. Into 4 other Swiss Webster mice.

Three days later on day ten, the gametocytes exflagellation events were checked under the microscope in dark-field on a covered blood drop. The exflagellation is visible after 10 min of waiting and there should be more than 3 per visible window. From this, the best 3 mice were anesthetized with Ketamine and fed for 20 min to one cage of mosquitos (approximately 200-300 female mosquitos). This procedure was terminal though subsequent CO_2 exposure and decapitation. The blood was then collected via cardiac puncture from the mouse to maintain the frozen blood stocks for new infections. The blood was diluted with Heparin to prevent clotting and Alsever's Solution (A3551 Sigma) containing 10% Glycerol additive to prevent crystallization and sporozoite death during the freezing and thawing process.

On day twenty the midguts containing the oocysts were extracted out of 10 mosquitos and were rated from 1 to 3 according to their oocysts burden and to give an idea if the cage will have a high yield on sporozoites. The dissection of the remaining mosquitos can be done between day twenty-four and twenty-eight, where most of the sporozoites traveled to the salivary glands of the mosquitos.

3.2.2 Giemsa stained blood smears for determining patency and parasitemia

Counting the parasitemia in mice is possible through Giemsa staining of blood smears where a blood drop from the mouse tail on a slide that was wiped across the slide. After a few minutes, the slides were rinsed with Methanol and 10-20% Giemsa stain solution (Sigma Aldrich GS500; diluted in deionized water 1:10) was added for 10min, rinsed and dried.

Two times 10 frames were counted for infected cells (light microscope, 100x) and the parasitemia was calculated with the assumption that 10 Frames of one layer blood contained 2000 red blood cells (RBC). Therefore the infected blood cells are divided by 2000 RBC and multiplied by 100 that gave the %of parasitemia.

Giemsa colors the body of the parasites blue, the head violet and the actin/ cytoplasm in the red blood cell precursors (reticulocytes) blue. The mature red blood cells remain predominantly uncolored with some showing a shimmer of pink.

3.2.3 Dissection of mosquitos and preparation of sporozoite injection

Two weeks after the mosquito's blood meal the salivary glands containing the sporozoites were taken out and injected on the same day into the mice.

The dissection procedure [13] started with the collection of the mosquitos out of the disposable cardboard cages through a suction tube into Ethanol. The dead mosquitos were washed with PBS and dissected under a microscope in a thin layer of cold Schneider Medium (Gibco™21720024 Schneider's Drosophila Sterile Medium). The heads were cut off and the salivary glands squeezed out of the upper body and collected into a 1,5 mL tube and stored on ice.

The isolated salivary glands were grounded with a pestle and were spun down at 800 xg for 3 min. The supernatant was saved and the pellet resuspended in 200 µL fresh Schneiders Medium step. This step was repeated once.

A 10 µL of the sporozoite solution (1:10) were analyzed in a hemocytometer after 15 min resting time (light microscope, 40x) All four grits were counted and in consideration of dilution factor, the volume of sporozoite solution and sporozoite counts, the total amount of sporozoites could be determined.

Ideal numbers for an experiment are more than 10 000 sporozoites per mosquito. In the case of only 5000 sporozoites per mosquito, it has been shown that the infection rate of the sporozoites is low. [78]

The sporozoites solution was further diluted to the desired concentration that should be administered intravenously through orbital injection. The sporozoite load was approximately 10 000 up to 100 000 sporozoites per 100µL.

The control groups of the experiments receive uninfected salivary glands (“mock”) infections that are prepared the same way as the sporozoite injections.

3.3 Flow cytometry

Flow cytometry is a multi-parameter method to phenotype cell populations based on their size, shape and granularity, which is determined through forward and sideward scatter and specific characteristic markers which are labelled through fluorescently conjugated antibodies that bind to intracellular or surface proteins. The cells are focused in a sheath of fluid to analyze every single cell by passing different lasers and the scattered light is filtered and detected in different PMTs (photomultiplier detectors).

The flow cytometer that was used was an LSRII and the applied laser and filter configurations can be found in Appendix 3.

The design of an appropriate flow panel requires knowledge about the phenotype of the desired cell which should be analyzed. The expression of specific markers at the time point of the cell isolation and the abundance of that marker on the cell must be known.

Based on that knowledge the right antibody conjugated fluorophores have to be chosen. The highly expressed markers should be labelled by a less bright fluorophore (=colors) than non-abundant ones. Additionally, it must be taken into consideration that the fluorophores should not have that many overlapping spectrums with other colors because it will not be able to compensate out the spillover signal from these detectors (channels).

The brightness of the fluorophores can be determined through Stain index or online tables that show the relative brightness from the fluorophores to each other.

As a tool, the online BD spectrum viewer (http://www.bdbiosciences.com/us/s/spectrumviewer) and BD Biosciences Relative Fluorochrome Brightness sheet was used for developing a new panel.

Controls

The usage of a working flow panel has to be tested on cell samples that contain all the included markers for proving that the antibody is binding and the fluorophore is still emitting. Further on the flow should always include controls to verify the reliability of the analysis.

- The **single stain (SS) controls** contain just one color to adjust the laser voltages at the beginning of the experiment and to create a compensation matrix for the flow data analysis that allows calculating the spillover of the other fluorophore's emission spectrums out of the actually measured spectrum.
- The **Full Minus One controls (FMOs)** are need to identify and gate around the right cell populations in the flow analysis. For this reason, the controls have to be the same cells as the actually measured cell samples and have to be treated the same way.
- A **sample without staining (blank control)** has to be included as well, to adjust the forward and sideward scatter and to have control of background staining.

Flow data analysis

The generated waw data was analysed in the FlowJo V10 software. The compensation was applied through a compensation matrix and based on the FMO controls the selected gates for the populations were determined.

3.3.1 Extracting lymphocytes out of liver and spleen

The lymphocytes have to be extracted the same day as the flow cytometry analysis takes place.

The required solutions for one mouse are 100mL flow buffer (1x PBS (10 mM phosphate, 137 mM NaCl and 2.7 mM, KCl, pH 7,4) and 2% FBS (Fetal bovine serum) and 1mM EDTA (SigmaAldrich; E7889)), 35 mL Wash buffer (1x PBS, 4% FBS, 0,5 mM EDTA), 10 mL Perfusion buffer (), Collagenase buffer () with 5 mg Collagenase, ,1, 67 mL OptiPrep™ Density Gradient Medium (Sigma Aldrich, D1556), 3 mL ACK buffer (150 mM Ammonium Chloride, 10 mM Potassium Bicarbonate, 0,01 mM EDTA)

a. Mouse organ extraction

The mice were anesthetized with 300µL of Ketamine solution and dissected (the abdominal skin and peritoneal membrane were cut open while the mouse was fixed on a Styrofoam pad with needles) so that the liver and spleen can be extracted. The liver was either perfused before (Pump perfusion buffer and collagenase buffer with tube and a 24G catheter on its end into the portal vein and the *Vena cava*) or the liver was just soaked in collagenase solution (5 mg collagenase in 10 ml collagenase buffer) for 4 min, whereas the spleen was just cut out.

The removed liver and the spleen were strained into Pedri-dishes through a sieve (100 µm/white <. 70µm) with a 10 mL syringe punch and were put into 50mL conical tubes on ice (30mL Wash buffer for liver and 5 mL for spleen).

b. Lymphocyte extraction from livers [79]

The ground and the sieved liver solution was spun down at 50 xg for 2min (to get rid of the hepatocytes) and the supernatant with the desired lymphocytes was transferred to a new 50 mL conical tube. The supernatant as spun down at 500 xg for 5 min (4°C) and resuspended in 2,5 mL 1x PBS and transferred to a 15 mL conical tube with 2,5 mL of 40 % OptiPrep solution (1,67ml OptiPrep density gradient medium/ 0,58ml 10x PBS/0,25ml purified water). The solution was overlayed with 1x PBS and carefully placed in the centrifuge. At 1500 xg with the settings of acceleration on 9 and a deceleration setting of 0 the cells were spun for 25 min. A thin layer in the two phases should be visible after the centrifugation and this was removed with 1ml Pipette and mixed with 5 mL flow buffer. The cells were washed one more time (spun down at 500 xg, discard the supernatant and the cells resuspended in 1 mL flow buffer).

c. Lymphocyte extraction from spleens

Red blood cell lysis was conducted through adding 3mL of the ACK buffer to the ground and sieved spleen solution and after 7min the tube was filled up with 20ml flow buffer and spun down at 500 xg for 5min and resuspended in 5 mL flow buffer.

d. Counting the cells

The liver cells were diluted 1:10 and the spleen cells 1:100 and were counted in a hemocytometer. Two fields out of four were counted and the cell number determined through the mean out of counts multiplied by the dilution factor and 10^4 to get the number of cells per mL.

3.3.2 Staining of viable leucocytes

After the lymphocyte cell extraction from liver and spleen, approximately 2-3 million cells were transferred to a 96-well plate and spun down at a speed of 500 xg for 5 min to get rid of the supernatant. The prepared Fc block solution (1,4 µL Fc block AB + 48,6 µL Flow Buffer) was added to each well and kept at room temperature for 30 min. Two million of the splenocytes were used for the single stains and were transferred to flow tubes and stained with 0,7 µL of flow antibody. 50 µL of the master mix solution is added X times to the 96-well plate, that contains (0,7 µL*X of each antibody + [50-(0,7*X)*amount of total colors] µL flow buffer and the cells were stored on ice. At the same time, the 50 µL of FMO mix was also added to the appropriate wells [0,7 µL* (amount of all colours-1) + rest flow buffer].

After the incubation the plate as spin down at 500 xg, the supernatant removed and the cells resuspended in 100 µL of flow buffer. This step was repeated 2 more times and in the end, the cells were resuspended in 200 µL flow buffer. 100 µL of flow buffer was added to the single stains to a have a total volume of 200 µL.

3.3.3 Flow panel development

Flow panel for CXCR3+ expressing cells

A detailed technical description of the CXCR3+ cells (CD4+,CD8+, NK, NKT, pDC) flow panel is listed in Table 1.

Table 1: Detailed overview of CXC3+ cell flow panel

Marker	Fluorophore	Laser (Excitation wavelength)	Single stains	Vendor/ Clone	Amount [µL]
		FSC	-	-	
		SSC	-	-	
B220	Per CP Cy5.5	Blue (488nm)	Same	Biolegend/ RA3-6B2	0,7
CD3	APC Cy7	Red (633nm)	Same	Biolegend/17A2	0,7
CD4	BV605	Violett (407nm)	Same	Biolegend/ RM4-5	0,7
CD8	BV785	Violett (407nm)	Same	Biolegend/53-6.7	0,7
Dx5 (CD49b)	PE Cy7	Green (532nm)	CD4	Biolegend/ Dx5	0,7
Bst2/PDCA-1	APC	Red (633nm)	CD4	Biolegend/927	0,7
Ly6c	BV421	Violett (407nm)	CD4	Biolegend/HK1.4	0,7
				All single stains: Biolegend/ GK1.5	0,7

The final test was conducted on a naïve C57BL/6J mouse and a 50 000 FabB/F sporozoites infected mouse (same treatment as in the further experiments).

Flow panel for liver Trm cells

A detailed technical description of the liver resident memory CD8+ T cell flow panel is listed in Table 2.

Table 2: Detailed overview of liver-resident memory CD8+ T cell flow panel

Marker	**Fluorophore**	**Laser (Excitation wavelength)**	**Single stains**	**Vendor /Clone**	**Amount (µL)**
FSC			-		
SSC			-		
CD19	BV785	Violet (407nm)	Same	Biolegend/6D5	0,7
CD3	APC-Cy7	Red (633nm)	Same	Biolegend/17A2	0,7
CD4	BV605	Violet (407nm)	Same	Biolegend/ RM4-5	0,7
CD8	AF488	Blue (488nm)	Same	Biolegend/53-6.7	0,7
CXCR3	BV421	Violet (407nm)	CD4	Biolegend/ CXCR3-173	0,7
CXCR6	PE	Green (532nm)	CD4	Biolegend/ SA051D1	2
CD69	APC	Red (633nm)	CD4	Biolegend/H1.2F3	1,4
CD44	PerCP Cy5.5	Blue (488nm)	CD4	Biolegend/IM7	0,7
CD62L	PE-Cy7	Green (532nm)	CD4	Biolegend/MEL-14	0,7
				All single stains: Biolegend/ GK1.5	

The final test was conducted on lymphocytes of a naïve C57BL/6J mouse and three times FabB/F immunized and challenged C57BL/6J mouse (6 weeks post challenge).

3.4 *In vivo* bioluminescent imaging (IVIS)

The IVIS (*in vivo* imaging system) allows taking whole body images of up to 5 living mice. The main idea is to measure the bioluminescence or fluorescence signal in anesthetized mice through a sensitive CCD camera.

The design of GFP and luciferase-expressing wildtype *P. yoelii* allows examining a wild-type parasite infection in differently treated mice. If the *Py* GFP-Luc parasites were able to establish and replicate successfully in the liver, a strong signal would be visible. Therefore the mice were analyzed in the IVIS chamber 42 to 44 hours after infection because at that time-point the sporozoites should have entered the liver. The secondary infection allowed evaluating the functional response of the immune system at the time of *Py* GFPLuc challenge. [24] In the case of immunized C57BL/6 mice, they can control the liver burden, whereas nontreated C57BL/6 mice cannot inhibit secondary liver infection and show a high signal in the IVIS.

Shortly before, the mice were put into the IVIS chamber on the platform, the hair was removed from their abdominal and they were anesthetized in an isoflurane chamber. Using the bioluminescence measurement, 100 µL of frozen Luciferin ((D-Luciferin, Potassium Salt from Goldbio; CAS 115144-35-9),) was injected intraperitoneally to activate the bioluminescence reaction of the Luciferase in the presence of ATP. The bioluminescence pictures were acquired after an exposure time of 3 min and the readout of the bioluminescence was performed by using the region of interest (ROI) settings of the Living Image 3.0 software. The circles of the ROI tools were drawn around the upper abdominal area, where the liver is located. The rainbow scale was shown in radiance (p/s/cm^2/sr) and the results were based on the readout of total flux (photons/second). The result could be further confirmed or disproved by blood-stage patency analysis.

3.5 CXCR3 antibody and fragmentation

Antibody: The used Armenian hamster CXCR3 antibody InVivoMAb anti-mouse CXCR3 (CD183) was obtained from BioXcell (BE0249). The antibody binds to the CXR3 receptor and blocks CXCL10 and CXCL11 from binding, however not CXCL9. The antibody showed depletion effects of CXCR3+ cells *in-vivo*. [80] Therefore the cleavage of the antibody into fab and $(fab)_2$ fragments was an approach to avoid the Fc mediated cell death.

Fragmentation Kits: Cleaving endopeptidases are commercially available in kits that use immobilized enzymes on agarose beads. In this experiments the immobilized pepsin resin from Thermo Fisher (20343 Immobilized Pepsin -Agarose Resin) and the Kits from Thermo Fisher (44985 Pierce™ Fab Preparation Kit-Papain) and G-Biosciences (786-1276 Fab & F(ab)2 Fragmentation of Mouse IgG1 (Ficin) with Protein G) are used to cleave the CXCR3 antibody.

3.5.1 Pepsin

The digestion of the CXCR3 antibody was followed the manual "Pierce™ $F(ab')_2$ Micro Preparation Kit", (manufacture's manual, online available), without doing the purification section (D). Additionally, the room temperature or 37°C used digestion buffer was a 20mM sodium acetate buffer ranged from pH 4,4, 4,5, 5 and 5,5 and aliquots are removed from the digestion tube after 2h, 2.15h/2.30h/2.45h, 3h,4h,6h,8h in multiple runs. A load of antibody ranged between 100 µg.

The first run just included the digestions times range from 2h, 3h, 4h, 6h until 8h. The second attempt the antibody was incubated just for 2h15min, 2.30min, 2h 45min and for 3h and in the digestion in buffer with pH 5 for 2h, 2h30 and 3h. The third attempt tested for digestion buffer pH 5 and pH 5,5 each incubated for 4h,5h and 6h with immobilized pepsin and 100 µg antibody on room temperature and 37°C.

Analysis of fragments

- SDS PAGE (sodium dodecyl sulfate-polyacrylamide gel electrophoresis)

The antibody fragments were tested with SDS-PAGE if they have been cut into the right sizes. A total sample of 20µL (containing 5-15 µg total protein, measured previously by Thermo Scientific™ NanoDrop™ spectrophotometer analysis) was mixed with 5 µL sample buffer (4x Lammli buffer with (reducing conditions) or without β-mercaptoethanol),(native conditions). In case of reducing conditions, the Lammli Sample solution is incubated at 100°C for 3 min. The mixture was loaded onto polyacrylamide gels (Invitrogen; ™NuPAGE™ Protein Gels, 1.0 mm, 15-well 4-12% NuPage Bis-Tris; NP0323BOX) in 1x NuPage buffer (Invitrogen;™ NuPAGE™ MOPS SDS Running Buffer (20X); NP0001). The SDS-PAGE was carried out at a voltage of 80 volts for 30 minutes and then 120V for 1,5h.

The standard protein marker from Biorad (cat. #161-0318) with a molecular weight range between 10 and 200 kDa was used for evaluating the size of the samples. After the run the gel was washed in deionized water for 10 min and stained with Coomassie blue (Invitrogen LC6060).

3.5.2 Ficin

The fragmentation are conducted according to the manual from G-Biosciences “Fab & F(ab)2 Fragmentation of Mouse IgG1” (manufacture’s manual, online available). The used cysteine amount was 1,76 mg in 10 mL digestion buffer. The fc part was cut into small pieces and a following affinity chromatography step (Protein G) separated the digested from the undigested antibody.

The incubation mix load was 950 µg incubated for 24, 26, 30, 32h and at each time points aliquots were taken and then purified with a Protein G column.

Analysis of fragments

- SDS PAGE (sodium dodecyl sulfate-polyacrylamide gel electrophoresis)

As described in Pepsin digest (native conditions).

3.5.3 Papain

The digestion was conducted according the “Pierce™ Fab Preparation Kit” manual (manufacture’s manual, online available). Papain produced two 50 kDa fab fragments and an intact Fc part. Non-digested IgG and the Fc part were separated through a Protein A column purification. The Fc part was binding to the Protein A resin and the Fab fragments went through.

Analysis of fragments

- SDS PAGE (sodium dodecyl sulfate-polyacrylamide gel electrophoresis)

As described in Pepsin digest (denaturating conditions).

- Analysis of binding capacity by flow cytometry analysis

After the CXCR3 antibody fragmentation, the fragments were characterized for their binding capacity in comparison to the undigested antibody.

Therefore a flow cytometer based analysis was developed in which isolated lymphocytes from liver and spleen were used (isolation procedure is described in chapter 3)

Two dissected C57BL6 mice were obtained from Jackson Laboratory (00664) and were treated with 10 000 *Py* GFPLuc sporozoites 20 days before the isolation. 2,5 * 10^6 splenocytes and liver lymphocytes were transferred into a 96 well plate and each well was treated with 1,4 µL Fc block (TruStain FcX™ (anti-mouse CD16/32) Antibody; BioLegend, 101319) plus 48,6 µL Flow buffer (described in chapter 3) and been kept on room temperature for 30 min.

After the cells were washed two times with flow buffer, the liver cells were incubated with no antibody and with the high concentration of 28 µg of whole antibody and fab fragments.

The next step was the fixation of the cells through 4% formaldehyde in the Fixation/Permeabilization solution. Therefore 96-well plate was spun down at 500 xg; the supernatant was removed, were resuspended in 100 µL of the fixation buffer. After 20 min the cells were washed two times with 1x wash/permeabilization buffer (BD Cytofix/Cytoperm™ Fixation/Permeabilization Solution Kit, 554714) and in the end they were resuspended in 100 µL of the staining solutions of the Mastermix (0,7 µL of: Brilliant violet conjugated anti-mouse CD19 (Biolegend, clone:6D5), Brilliant violet conjugated anti-mouse CD3 (Biolegend, clone: 17A2), PE-conjugated anti-mouse CD4 (Biolegend, clone: GK1.5) Alexa Fluor 488 conjugated anti-mouse CD8 (eBioscience, clone:53-6.7) and APC conjugated anti-mouse CXCR3 (Biolegend, clone: CXCR3-173)), The FMOs and single stains (all fluorophores are conjugated to CD4; Biolegend clone GK1.5) are added to splenocytes because the liver did not contain enough cells for the FMO controls and instead of CXCR3-APC; APC conjugated anti-mouse from Biolegend clone: GK1.5 is used.

3.6 Experiments

This section covers the experimental setup for the experiments that investigate the impact of CXCR3 and its chemokines in the adaptive (Protection experiments) and innate immune response to control a *Py* GFPLuc wild-type infection (challenge).

3.6.1 Role of CXCR3 in the adaptive immune control

a. Protection experiment (CXCR3 antibody treatment)

Mice: In this experiment, 8-week old C57Bl/6J were used (described in 3.1 Mice).

Time points of immunization and antibody administration: The sporozoite immunization were prepared according to 3.2.3. The 50 000 FabB/F sporozoite injections or uninfected salivary glands (mock) injections (Table 3) were administered three weeks apart from each other. After four weeks post Boost 2, all mice received a 10 000 *Py* GFP-Luc challenge injection, whereas 3 days prior challenge 200 µg and one day before, or an IgG isotype control antibody was injected (Figure 5, indicated by black arrows in the timeline). The CXCR3 antibody bound to the receptor and depleted the CXCR3 expressing cells.

The chosen time points and amounts of CXCR3 antibody injection were based on the papers of [58][81] as the same CXCR3 antibody was injected to deplete CXCR3+ cells.

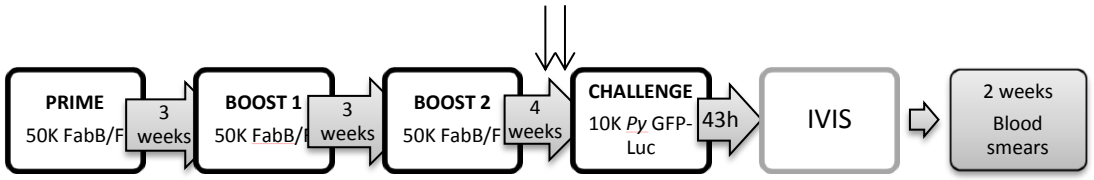

Figure 5: Schematic immunization time line for protection experiment in CXCR3 antibody treated C57BL/6J mice

Analysis by IVIS and Giemsa stained blood smears. The IVIS analysis was conducted 43h post challenge (as described in 3.4) and patency was determined of blood smears (as described in chapter 3.2.2) analysis through two weeks.

Table 3: Groups for protection and flow characterization experiment

Group	Treatment + Antibodies		
1	Mock	+ Isotype IgG control	+ GFPLuc challenge
2	50k/50K/50K FabB/F	+ Isotype IgG control	+ GFPLuc challenge
3	Mock	+ αCXCR3 antibody	+ GFPLuc challenge
4	50k/50K/50K FabB/F	+ αCXCR3 antibody	+ GFPLuc challenge

b. Protection experiment (CXCR3 knockout mice)

Mice: In this experiment, 8 week old C57Bl/6J and CXCR3 knockout mice were used (described in 3.1 Mice).

Time points of immunization: The sporozoite immunization were prepared which is described in 3.2.3. The 50 000 FabB/F sporozoites injections were administered three weeks apart from each other into the FabB/F treated groups (Table 4). After four weeks post boost 2, all mice received 10 000 *Py* GFP-Luc injection. The overview of the immunization strategy is shown in Figure 6.

Figure 6: Schematic immunization timeline for protection in CXCR3 knockout mice

Analysis by IVIS and Giemsa stained blood smears: The IVIS analysis was conducted 43h post challenge (as described in 3.4) and patency was determined of blood smears (as described in 3.2.2) analysis through two weeks.

Table 4: Groups for protection analysis (CXCR3 knockout mice)

Group	Mouse strain + Treatment		
1	C57Bl/6J	+ Mock	+ GFPLuc challenge
2	C57Bl/6J	+ 50k/50K/50K FabB/F	+ GFPLuc challenge
3	CXCR3$^{-/-}$	+ Mock	+ GFPLuc challenge
4	CXCR3$^{-/-}$	50k/50K/50K FabB/F	+ GFPLuc challenge

3.6.2 Role of CXCR3 in the innate immune control and recruitment

Mice: In this experiment, 8 week old C57Bl/6J and 8-weeks old CXCR3 knockout mice from internal breed were used (described in 3.1 Mice)

Time points of immunization: The sporozoite immunization were prepared according to 3.2.3. and injected into the FabB/F treated groups (Table 5). The 100 000 FabB/F injection was administered 3 days before a 50 000 *Py* GFPLuc challenge (as shown in Figure 7).

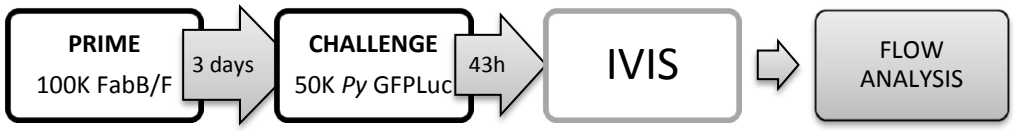

Figure 7: Schematic immunization timeline for innate immunity und recruitment experiment

Analysis by IVIS: The IVIS analysis was conducted 43h post challenge (as described in 3.4)

A following flow analysis evaluated the recruitment of immune cells to the liver

Liver perfusion and lymphocytes extraction: Immediately 3 mice per group were anesthetized and the liver was perfused and taken out and processed as described in the chapter 3.3.1. One spleen from a female mouse (group C57BL/6 +FabB/F) was cut out and processed as described in the chapter 3.

Flow panel analysis: The developed flow panel was used to detect the cell populations which express CXCR3+ in a wildtype mouse (Table 1). The analysis run on an LSRII flow cytometer and the data was analyzed in the FlowJo V10 software, compensation was applied through a compensation matrix and the gates around the populations are determined according to the FMO controls.

Table 5: Groups for the innate immunity und recruitment experiment (CXCR3 knockout mice)

Group	Mouse strain + Treatment		
1	C57Bl/6J	+ Mock	+ GFPLuc challenge
2	C57Bl/6J	+ 50k/50K/50K FabB/F	+ GFPLuc challenge
3	$CXCR3^{-/-}$	+ Mock	+ GFPLuc challenge
4	$CXCR3^{-/-}$	50k/50K/50K FabB/F	+ GFPLuc challenge

3.7 Statistics

The statistical analysis was conducted in Graph pad prism 5 software by a two-tailed Mann-Whitney-U-Test and an unpaired t-test with Welch's correction by comparing the two groups. The labeling of the figures followed the pattern:
Not significant (ns.): $p>0,05$; Significant: $*p<0,05$, $**p<0,01$

4 Results

4.1 Role of CXCR3 in the adaptive immune response

4.1.1 CXCR3 expression on antigen-experienced CD8+ memory T cells

Memory CD8+ T cells are critical for protection after GAP immunization [39]. Additionally in RAS immunized mice liver resident memory CD8+ T cells express CXCR3. Determining if this holds true after GAP immunization, C57BL/6 mice were immunized three times with FabB/F and examined CXCR3 expression on antigen-experienced CD8+ T cells and antigen-experienced CD4+ T cells 6 weeks after the last immunization.

The final test of the tissue resident memory T cell flow panel could show that CXCR3 is abundantly expressed on antigen-experienced CD8+memory T cells and on CD4+ memory T cells. On the one hand, the flow analysis it was to display if the flow panel was working and on the other hand it demonstrated that CXCR3 is expressed on memory CD8+ T cells, which are essential for the protection.

The analysis with the Trm cell flow panel showed that 80,2% of all antigen-experienced CD8+ memory T cells expressed the CXCR3 receptor after 6 weeks post challenge and three previous immunization with FabB/F (Figure 8).

Besides the interesting activated memory CD8+T cells for protection, the receptor was also highly abundant on 83,1% (Figure 8) of antigen-experienced CD4+ cells.

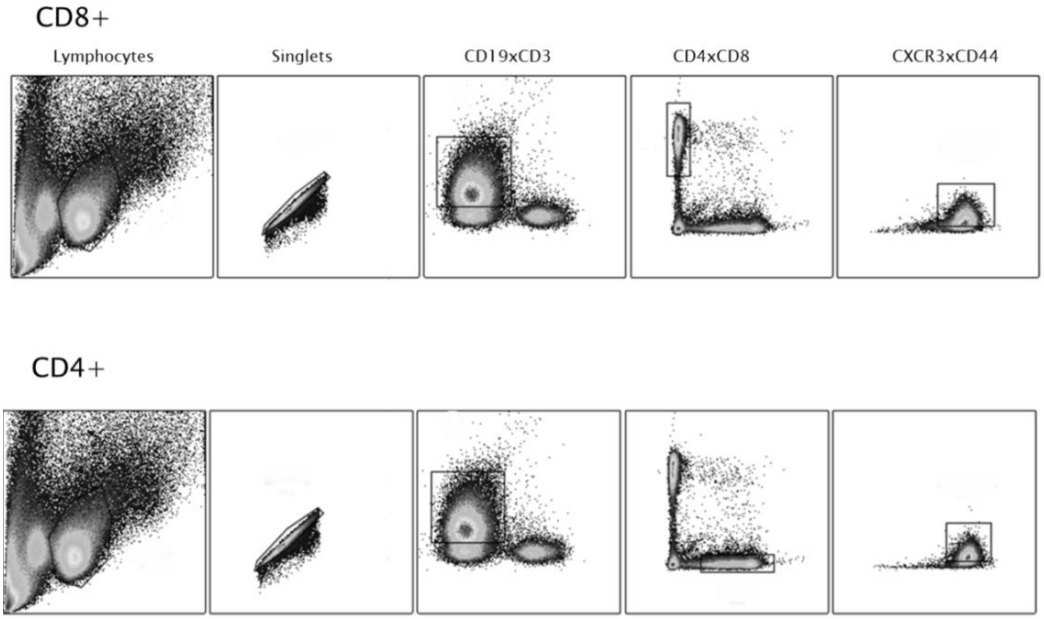

Figure 8: Flow plots of CD8+ and CD4+ liver lymphocytes out of immunized C57BL/6J mouse

Gating strategy for antigen-experienced CD8+ (upper row) and CD4+ cells (row of pictures below). The lymphocytes were detected via forward (FSC) versus sideward scatter (SSC) and out of that only the single cells were identified via SSC (area) vs. SSC (height). The CD8+ cell population was identified by the markers CD3+/CD19-/CD8+/CD4-/CD44+/ CXCR3 and the CD4+ cell population by the markers CD3+/CD19-/CD8-/CD4+/CD44+/ CXCR3 which is indicated in the headline of the single pictures of the top row. (X-axis vs. Y axis).

4.1.2 CXCR3+ tissue resident memory CD8+T cells are located in the liver

In RAS immunized mice, protection has been shown to be dependent on a population of CXCR3 expressing tissue resident cells in the liver. These cells are not present in other lymphoid organs such as the spleen or lymph node but establish residency in the liver to quickly eliminate infected hepatocytes. [58]

The Trm flow panel could also show that 6 weeks after three FabB/F immunization and a challenge, the establishment of a population of CXCR3+ liver resident memory CD8+ T cells in the liver, but not in the spleen, took place. The Trm cells were characterized by the markers CD3+, CD19-, CD8+, CD44+, CD62L-, CXCR6+, CD69+, CXCR3+ (Figure 9).

The total counts of the Trm cells are illustrated in Figure 10, where 26880 cells could be detected in the liver of the immunized mouse whereas there was no population visible in the spleen of the same mouse (545 cells). This implies that the Trm were truly resident in the liver and not in the spleen.

Moreover, it could be seen that the naïve mouse (figure 10) had only 1931 positive counts in the liver and 6 in the spleen that meant that the sporozoites infection triggered the establishment of the Trm cells.

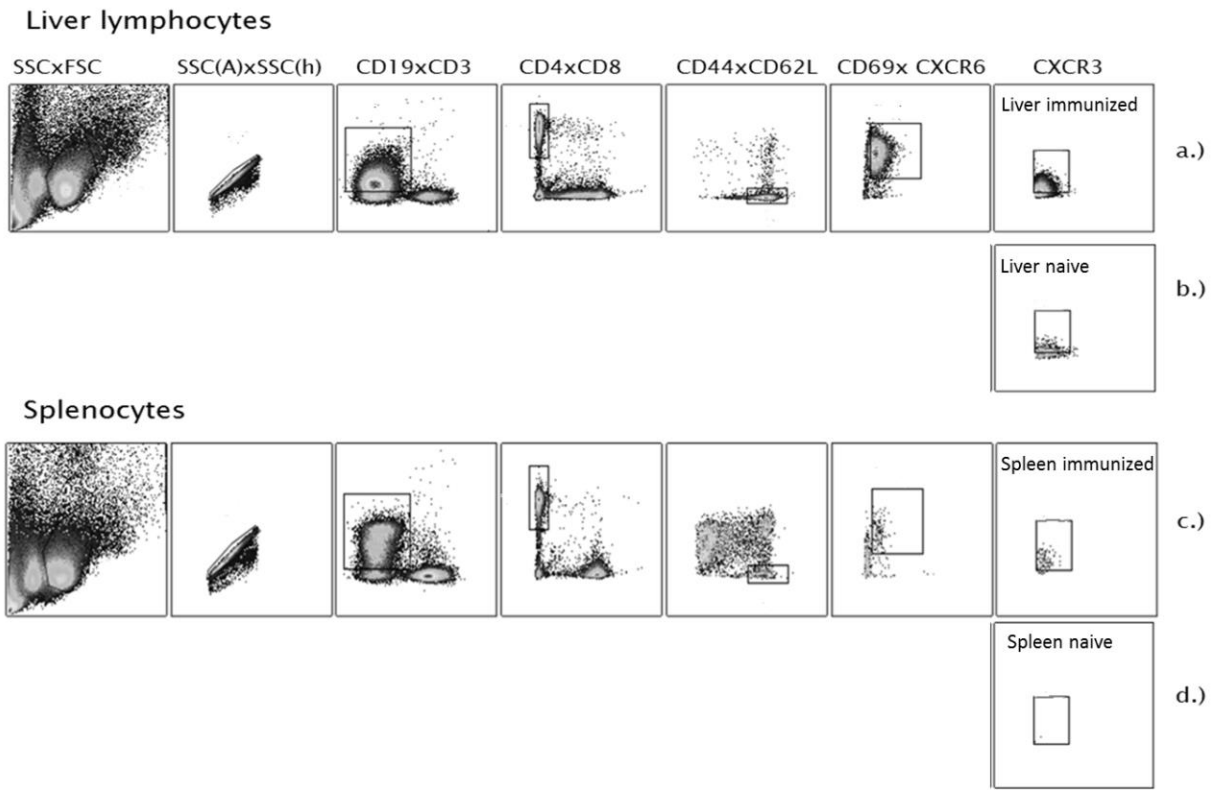

Figure 9: Flow plots of liver and spleen of immunized mouse and naïve mouse

Gating strategy for identifying liver resident memory CD8+ T cells in the liver and spleen of a naïve and an immunized C57BL/6J mouse. The lymphocytes were detected via forward (FSC) versus sideward scatter (SSC) and out of that only the single cells were identified via SSC (area) vs. SSC (height). The Trm cell population was identified by the markers CD3+/CD19-/CD8+/CD4-/CD44+/CD62L-/CXCR6/CD69+/CXCR3 which is indicated in the headline of the single pictures of the top row. (X axis vs. Y axis). a) Full gating strategy of liver CD8+ Trm cells out of a three times immunized and challenged mouse. b) Liver CD8+Trm cell population of a naïve mouse c.) Full gating strategy on splenocytes for a liver CD8+ Trm cell population out of a three times immunized and challenged mouse.d.) Splenocytes cell population that is + for liver Trm cells

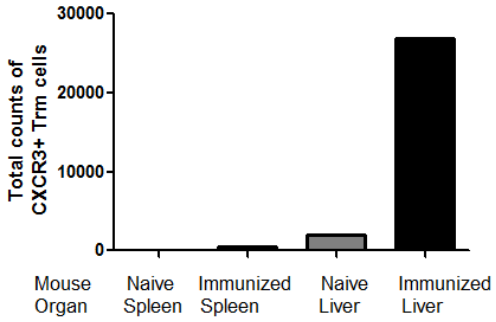

Figure 10: Total counts of liver-resident memory T cells in liver and spleen

X-axis: Treatment of the mouse and the analyzed organs were described. Each bar represents one the organ of mouse. Therefore error bars are missing due to sample size (x<3).

y-axis: Counts of Trm cell range from 0-30000 positive detected cells

4.1.3 Protection experiment (CXCR3 antibody treatment)

Based on the findings that CXCR3 is expressed on the antigen-experienced memory CD8+ T cells in the liver, which were proposed to mediate protection, this experiment should confirm that the depletion of the CXCR3+ cells mediated through a CXCR3 antibody treatment at the time point of challenge leads to a loss in protection. This was investigated by an IVIS analysis and patency determination by Giemsa stained blood smears.

The CXCR3 antibody is known to deplete only CXCR3+ cells in the liver, that are crawling over epithelial surfaces to be depleted by Kupfer cells by ripping off the trailing edge of the cells. [81] This supports the result that the protection is lost through depletion of the Trm cells which are crawling over the epithelial surfaces of the sinusoids.

Protection is lost in CXCR3 antibody treated immunized C57BL/6J mice

The IVIS analysis of the three times immunized and CXCR3 antibody treated C57BL/6 mice showed that the protection against a following GFPLuc wildtype challenge is lost due to the depletion of the CXCR3+ expressing cell population at the time of challenge.

Representative images of luminescence in livers of mice 43 h post challenge are shown in Figure 11. Scales were expressed in radiance (p/s/cm^2/sr). Measurements were framed by ROI (region of interest) circles that include the area where the liver was located and the signal appeared.

The quantification of bioluminescent signal in total flux (p/s) from mice at 43 h post challenge could be demonstrated in Figure 11. The appertaining table can be found in Appendix 6.

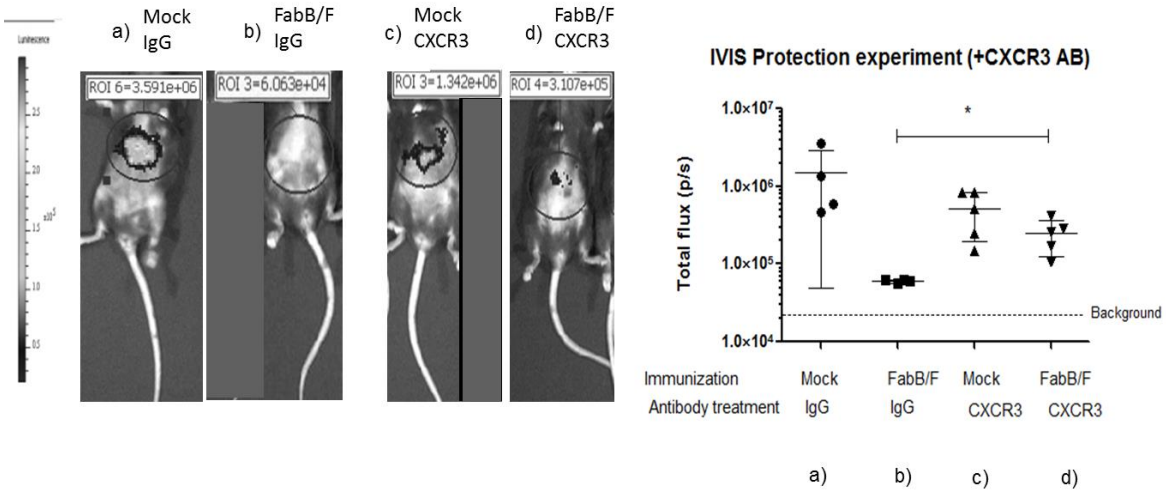

Figure 11: IVIS protection data (CXCR3 antibody)

Pictures (left) ROI framed circles to determine the radiance in p/s/cm2/sr; Black/ grey clouds indicated high liver burden (visible in a,c,d)

Graph (right): The x-axis describes the immunization with FabB/F or mock and the correlated antibody treatments below. The y-axis plotted the quantification of the bioluminescent signal in total flux (photons/second) at a range from 10^4 until 10^7. The scattered line defined the background level signal. Each data point represents an individual mouse (4 mice in the IgG-treated groups, 5 mice in the CXCR3 antibody treated groups). Bar graphs represent the mean ± SD of the data. The statistical analysis was conducted in Graph pad prism 5 software through a two-tailed Mann-Whitney-U-Test by comparing the immunized groups. Asterisk indicates statistical significance between the control groups Mock/IgG group and the immunized FabB/F/IgG group, whereas the other groups are not significant. (*p = 0.0159)

The Mock+ IgG group showed the highest bioluminescence signals (a) that imply that the mouse was not protected against the following *Py* GFPLuc wildtype infection after three mock (uninfected mosquito glands) injections. In b) the immunized mice with FabbB/F did not show any signal as expected because they are supposed to be protected against the wildtype *Py* GFPLuc infection after three FabB/F immunization. Out a) and b) it could be concluded that the IVIS worked because the positive and negative control showed a 10^2 difference in the bioluminescent signal. The Mock+ CXCR3 antibody control group (c) showed that they were comparable with the Mock + IgG group to exclude that the CXCR3 antibody itself influenced protection. The last group was the immunized FabB/F mice treated with the CXCR3 antibody that showed a reduced signal which was significant in comparison to the Immunized+IgG, in which the CXCR3+ expressing cells were present, which concluded that a protective cell population was reduced or eliminated, which are CXCR3 positive.

CXCR3 antibody treated mice became patent 5 days post challenge

The blood smears that were taken from each mouse and Giemsa stained every day for two weeks. The Giemsa stained slides were evaluated according to the egressed parasites from the liver into the blood. In case one single parasite was detected, the mouse was evaluated as positive (became patient). The following day was analyzed as well to prove that the mouse showed an increased parasitemia.

Therefore the patency analysis could confirm the result in the IVIS because the immunized mice which received the CXCR3 cell depleting antibody were patent after 5 days post challenge, whereas the immunized mouse which received an isotype IgG antibody was sterile protected until two weeks after challenge (day 17). The mock-treated controls became patent on day 4 (Mock+ IgG) and day 5 (Mock+CXCR3) (Figure 12).

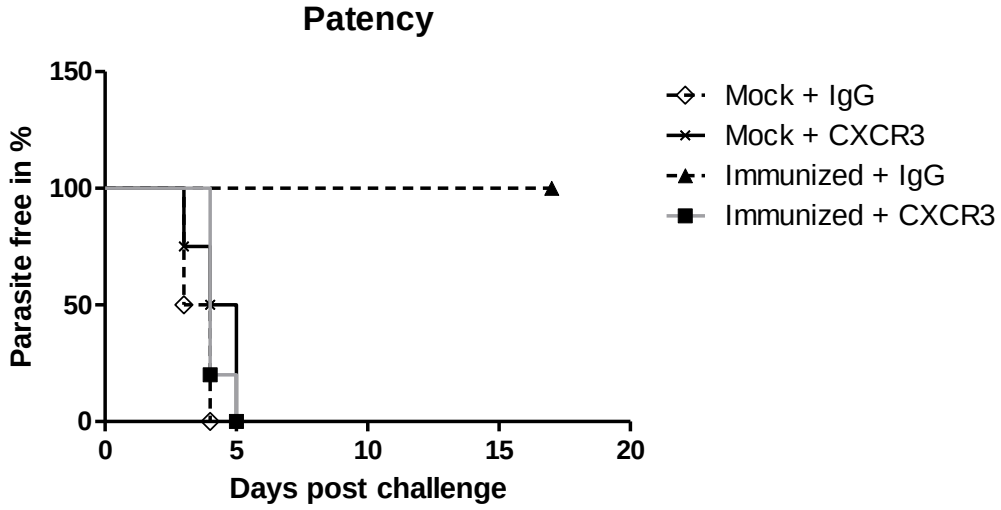

Figure 12: Patency after IVIS analysis in protection experiment (CXCR3 antibody treatment)

On the x-axis the days after post challenge are plotted and the y-axis represents the % of parasitemia free mice. Each line represents a group of 4 to 5 mice. The symbols indicate the group (seen in figure legend) and are present on the corners to follow up the lines. The grey line with full squares highlights the FabB/F immunized mice treated with CXCR3 antibody.

The delay of one day in patency in the CXCR3 antibody treated groups was consistent with the bioluminescence data that also suggested that the mice treated with CXCR3 antibody show a less pronounced signal in comparison to the IgG isotype control antibody. The reduced bioluminescence signal implied a lower liver burden through fewer parasites in the liver after 43h that needed one day longer to establish a blood stage. Therefore it can be said that the depletion of CXCR3 + cells had a strong impact on protection.

Additionally, confirming that the dosage of CXCR3 antibody of 250µg and 100 µg/mouse, three and one days before the challenge was efficient, the serum of the mice should be analyzed by an ELISA (enzyme-linked immunosorbent assay) one week before challenge and on the day of challenge with a following flow analysis. The combined data would show the correlation between antibody titer and the % of depleted cytotoxic memory T cells in vivo.

4.1.4 Protection experiment (CXCR3 knockout mice)

The flow panel development showed that CXCR3 receptor is expressed on activated CD8+ T cells and Trm cells and the protection experiment with the CXCR3 antibody demonstrated that a CXCR3 expressing cell population is responsible for the protection against a wildtype *Py* GFPLuc infection.
The same experiment was conducted in CXCR3 knockout mice. The purpose was to identify if CXCR3 receptor is involved in the protective response after three immunization and a following wildtype *Py* challenge. This was investigated by an IVIS analysis with a following patency determination by Giemsa stained blood smears.

FabB/F immunized CXCR3$^{-/-}$ mice showed protection against *Py* GFPLuc challenge

Surprisingly, the IVIS data suggested that the immunized CXCR3 knockout mice did not show a loss in protection as it would be expected if CXCR3 would be involved in any process of recruitment, establishment and protection (Figure 13). The appertaining table can be found in Appendix 7.

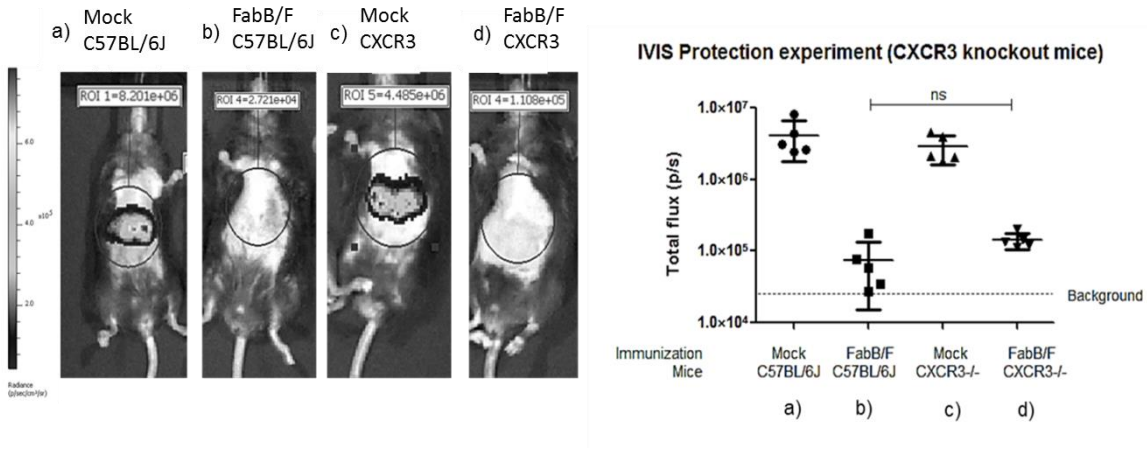

Figure 13: IVIS innate immunity data (CXCR3 antibody)

Left: ROI framed circles to determine the radiance in p/s/cm2/sr; Black/ grey clouds indicated high liver burden (visible in a, c)

Right: The x-axis describes the immunization with FabB/F or mock and the used mouse strain below. The letters (a-d) are matching with the groups from pictures from the left. The y-axis plotted the quantification of the bioluminescent signal in total flux (photons/second) at a range from 10^4 until 10^7. The scattered line defined the background level signal. Each data symbol represents an individual mouse (5 mice in each group). Bar graphs represent the mean ± SD of the data. The statistical analysis was conducted in Graph pad prism 5 software through a two-tailed Mann-Whitney-U-Test by comparing the two immunized groups. There were no significant differences measurable between the groups (ns. Not significant: p>0,05)

The mock-treated wildtype C57BL/6 mice (received uninfected mosquito salivary glands) showed the highest bioluminescence signals in (a) that imply that the mouse was not protected against the following *Py* GFPLuc wildtype infection. However, the immunized C57BL/6J group showed a 10^2 reduction in the bioluminescent signal in comparison to the mock. The mock-treated CXCR3 knockout mice control group (c) showed that they were comparable with the mock-infected wildtype mice to exclude that the absence of the CXCR3 receptor influenced the protection. The interesting group of three FabB/F immunized CXCR3 knockout mice (d) showed no significant difference to the FabB/F immunized wildtype mice, which concluded that the CXCR3 receptor might not be necessary for the protection against a following wildtype infection after one month post last FabB/F immunization.

FabB/F immunized CXCR3$^{-/-}$ showed sterile protection against *Py* GFPLuc challenge

After the IVIS was conducted the blood smears were taken from each mouse and Giemsa stained every day for two weeks. The Giemsa stained slides were evaluated according to the parasitemia load in the blood. In case one single parasite was detected, the mouse was evaluated as positive (became patient). The following day was analyzed as well to prove that the mouse showed an increased parasitemia.

The patency analysis could confirm the result in the IVIS because mock injected mice (CXCR3 knockout and C57BL/6J) showed a high liver burden and became patent on day 3. Whereas the immunized mice were sterile protected and no difference could be seen between the wildtype and CXCR3 knockout mice (Figure 14).

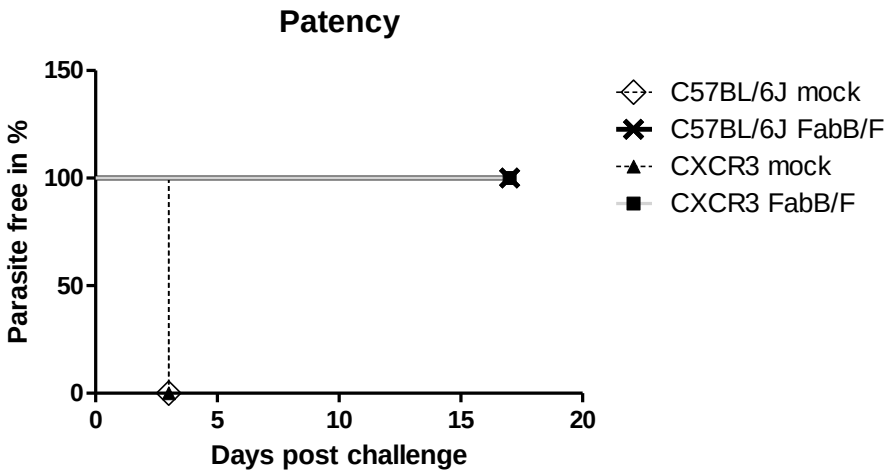

Figure 14: Patency after IVIS analysis in protection experiment (CXCR3 knockout mice)

On the x-axis the days after post challenge are plotted and the y-axis represents the % of parasitemia free mice. Each line represents a group of 5 mice. The symbols at the end of a line indicate the mouse strain and treatment (seen in the figure legend). The grey line with full squares highlights the FabB/F immunized CXCR3 knockout mice whereas the full black line with the X demonstrate the wild-type immunized C57BL/6J mice and the dashed lines represent the mock-treated mice.

Therefore the impact of CXCR3 seemed to be not crucial for the protection against a *Py* GFPLuc challenge after three immunizations.

4.2 Role of CXCR3 in the innate immune response

4.2.1 Innate immune control experiment (CXCR3 knockout mice)

Even though the CXCR3 knockout mice experiment did not show a functional outcome in the adaptive immune response (memory T cell-mediated) the innate immune response to sporozoites is often differently mediated and has to be evaluated separately. Therefore the approach was started to look at the innate immune response in CXCR3 knockout mice, explicitly focusing at the NKT cells (control liver burden in innate immune response) and the recruitment of activated adaptive immune cells, like CD4+ and CD8+ cells. This was investigated through an IVIS and following multicolor flow analysis.

Fab/F infected CXCR3$^{-/-}$ mice are capable of controlling a secondary *Py* GFPLuc infection

The IVIS data suggested that there is no significant difference between the immunized C57BL/6J mice and the CXCR3 knockout mice (Figure 15).

Representative images of luminescence in livers of mice 43 h post challenge are shown in Figure 15 (left). Scales were expressed in radiance (p/s/cm^2/sr). Measurements were framed by ROI (region of interest) circles that include the area where the liver was located and the bioluminescence signal of the GFPLuc parasites appeared.

The quantification of bioluminescent signal in total flux (p/s) from mice at 43 h post challenge could be demonstrated in Figure 15. The appertaining table can be found in Appendix 8.

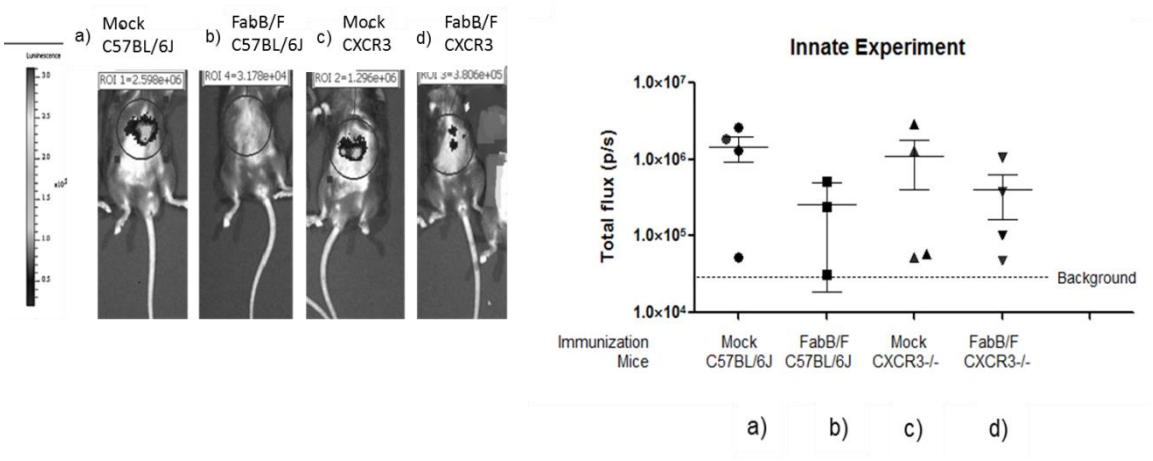

Figure 15: IVIS innate immunity data (CXCR3 antibody)

Left: ROI framed circles to determine the radiance in p/s/cm2/sr; Black/ grey clouds indicated high liver burden (visible in a, c,d)

Right: The x-axis describes the immunization with FabB/F or mock and the used mouse strain below. The letters (a-d) are matching with the groups from pictures from the left. The y-axis plotted the quantification of the bioluminescent signal in total flux (photons/second) at a range from 10^4 until 10^7. The scattered line defined the background level signal. Each data symbol represents an individual mouse (4 mice in each group). The black, grey, dark grey and white symbols indicate the concrete association to a particular mouse (black=female no.1, dark grey= female no. 2, grey=male no. 1, white= male no 2). Bar graphs represent the mean ± SD of the data. The statistical analysis was conducted in Graph pad prism 5 software through a two-tailed Mann-Whitney-U-Test by comparing the two immunized groups. There were no significant differences measurable between the groups (ns. not significant: p>0,05)

The mock-treated C57BL/6 group (received uninfected mosquito salivary glands) showed the highest bioluminescence signals in (a) that imply that the mouse was not protected against the following *Py* GFPLuc wildtype infection. However, the immunized C57BL/6J group showed a 10 fold reduction in the bioluminescent signal in comparison to the mock (which implies that the FabB/F injection was weak in comparison to the GFPLuc injection). The mock-treated CXCR3 knockout mice control group (c) showed that they were comparable with the mock-infected wildtype mice to exclude that the absence of the CXCR3 receptor influenced the protection. The interesting group of FabB/F treated CXCR3 knockout mice (d) showed no significant difference to the FabB/F treated wildtype mice, which concluded that the CXCR3 receptor might not be essential for the protection against a secondary wildtype infection after three days post FabB/F injection.

Reduction of liver recruited CD8+ T cells in the liver of CXCR3$^{-/-}$ mice after FabB/F and secondary GFPLuc challenge

The flow analysis showed that the only CXCR3 expressing cell population which was significantly altered were the CD8+ T cells, whereas no other cell population showed a significant difference between three immunized wildtype C57BL/6J and immunized CXCR3 knockout mice.

Immediately after the IVIS (43h), the mice were sacrificed; the livers were perfused and underwent a following lymphocytes extraction. The lymphocytes were counted and stained with the flow antibodies of the CXCR3+ expressing cells flow panel (Table 1) and all CXCR3+ cell populations were quantified (B cells, T cells, CD4+, CD8+, B cells, NK, NKT, pDc).

In Figure 16 and Figure 17 the gating strategy for the CD8+T cells and NKT cells is illustrated (CD8+ T cell population followed the staining pattern of CD3+/CD8+ and NKT cells were analyzed with the cell surface markers CD3+/CD49b). Therefore the immunized groups of C57BL/6J and CXCR3 knockout mice were compared for their abundance in the liver. The data demonstrated that only the CD8 + T cells were reduced in their recruitment to the liver, whereas the NKT cells were not (Figure 18).

The FMO controls should show that the gates were placed in the right way so that the real population was identified (figure 16 e.) and figure 17 e.)).

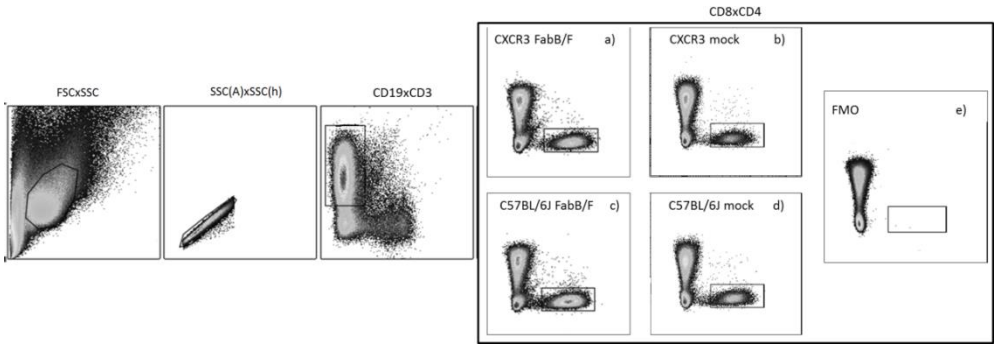

Figure 16: Gating strategy of CD8+ cells in mock and FabB/F treated CXCR3 knockout mice and C57BL/6J

The lymphocytes were detected via forward (FSC) versus sideward scatter (SSC) and out of that only the single cells were identified via SSC (area) vs. SSC (height). The CD8+ cell population was identified by the markers CD3+/CD8+ which is indicated in the headline of the framed pictures. (X-axis vs. Y-axis). a) CD8+T cell population of FabB/F injected CXCR3 knockout mice b) CD8+T cell population of mock injected CXCR3 knockout mice c) CD8+T cell population of FabB/F injected C57BL/6J mice d) CD8+T cell population of mock injected C57BL/6J mice e.) FMO control for CD8+ T cell population

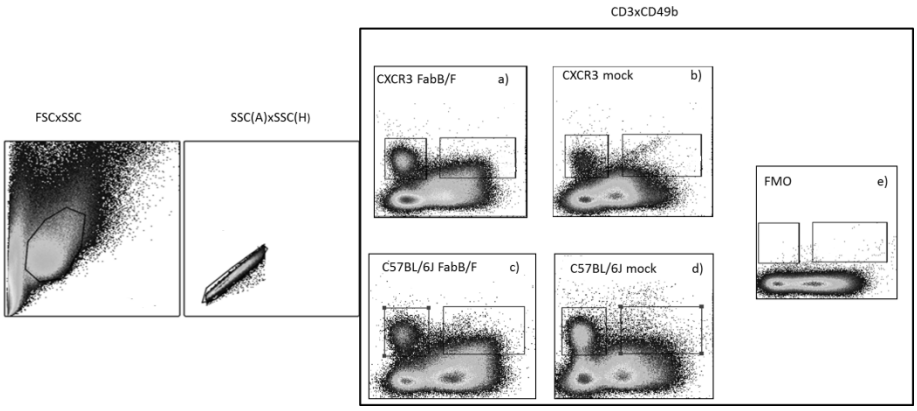

Figure 17: Gating strategy of NK and NKT cells in mock and FabB/F treated CXCR3 knockout mice and C57BL/6J

The lymphocytes were detected via forward (FSC) versus sideward scatter (SSC) and out of that only the single cells were identified via SSC (area) vs. SSC (height). The NK cell population was identified by the markers CD3-/CD49b+ and NKT cells with CD3+/CD49b+ which is indicated in the headline of the framed pictures. (X-axis vs. Y-axis). a) NKT cell population of FabB/F injected CXCR3 knockout mice b) NKT cell population of mock injected CXCR3 knockout mice c) NKT cell population of FabB/F injected C57BL/6J mice d) NKT cell population of mock injected C57BL/6J mice e.) FMO control for NKT cell population

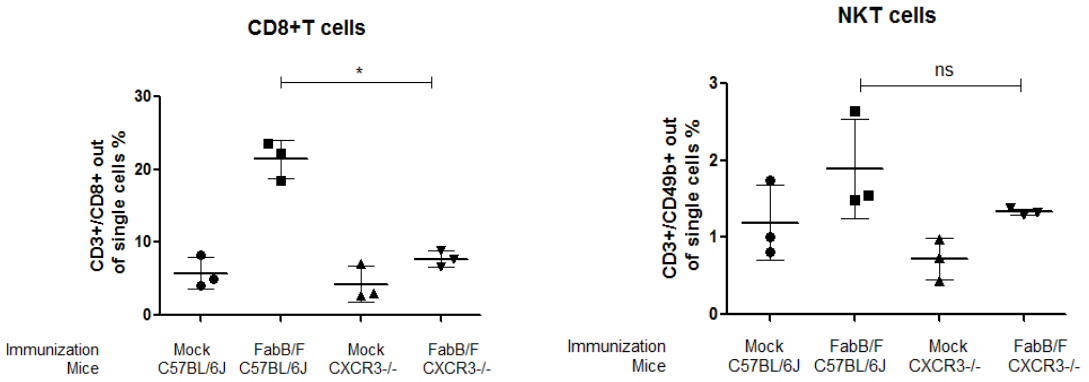

Figure 18: Flow cytometry analysis of CD8+ and NKT cells

X-axis: Immunization (mock=uninfected salivary glands; FabB/F treated mice) and used mice strain

Y-axis: Counts per 1 Mio single cells

Each data symbol represents an individual mouse (3 mice in each group). Bar graphs represent the mean ± SD of the data. The statistical analysis was conducted in Graph pad prism 5 software through an unpaired t-test with Welch's correction by comparing the two immunized groups. The asterisk indicates a significant difference in CD8+ T cell population. (* p= 0.0139). There was no significant differences measurable in NKT cells (ns: p>0.05; p= 0.2735)

The other graphs for the CXCR3+ expressing cells are shown in figure X. The T cells were characterized through the marker CD3, CD4+ T cell population followed the staining pattern of CD3+/B220-/CD4+, B cells were B220+/Ly6c-, NK cells were CD3-/Dx5+ and pDc showed the surface markers Ly6c/B220+/Bst2+ (Figure 19). There were no significant differences in the cell populations between FabB/F immunized wildtype and CXCR3 knockout mice. That concludes that these cell types were not affected in their recruitment to the liver by the absence of the CXCR3 receptor.

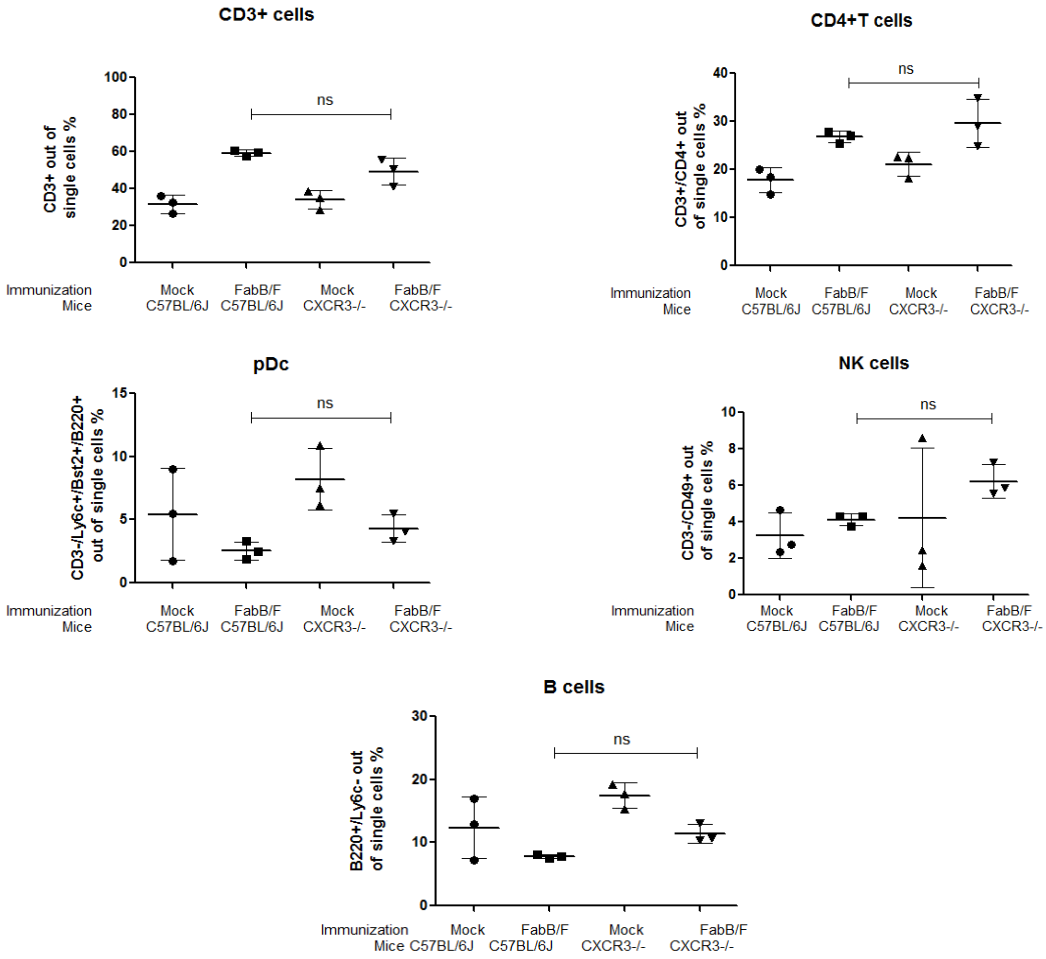

Figure 19: Flow cytometry analysis of CD3+, CD4+, B cells, pDc, NK cells

X-axis: Immunization (mock=uninfected salivary glands; FabB/F treated mice) and used mice strain

Y-axis: Counts per 1 Mio single cells

Each data symbol represents an individual mouse (3 mice in each group). Bar graphs represent the mean ± SD of the data. The statistical analysis was conducted in Graph pad prism 5 software through an unpaired t-test with Welch's correction by comparing the two immunized groups. No significant differences measurable between FabB/F treated groups (ns: p>0.05)

Taken the results of innate immune response and the recruitment together, the data seemed to be conclusive because it is known that only NKT cells have an impact on controlling secondary liver infection in the innate immune response, whereas CD8+T cells do not and therefore no elevation of the liver burden signal was visible. [10]

Even though the IVIS analysis showed outlier due to a weak FabB/f infection, the flow data showed relatively equally distributed sizes of cell population. So it can be concluded that the impact on the recruitment of the immune cells into the liver is less dependent on the number of sporozoites to see a difference in cell population size, it seemed to be more dependent on if the parasite was present or not.

4.3 CXCR3 digestion with pepsin, ficin and papain

The aim for the CXCR3 antibody fragmentation was to create a powerful tool to evaluate the influence of the chemokine system CXCR3 and its chemokines at different time points. Besides the evaluated priming (innate immune response and first adaptive immune response), it would give the opportunity to see if the receptor and its chemokines have an impact on the recruitment of immune cells into the liver, on the retention of these cells and further the protection against *Py* GFPLuc infection. The approach to cleave the CXCR3 antibody was to use the proteolytic enzymes pepsin, ficin and papain.

4.3.1 Pepsin

The fragmentation of the CXCR3 antibody with pepsin was not possible because of unspecific cleaving sites that fragmented the antibody completely.

SDS PAGE

The first attempt of the pepsin digestion showed that after 2h hardly any antibody is cleaved whereas after 3h the antibody is completely fragmented into 10 kDa fragments (Figure 20). Therefore an attempt was started to digest between 2h and 3h and showed that the fragmentation happened between 2.15 h and 2.30 h. The antibody was again cleaved completely into 10 kDa fragments. Even the positive control, a αCSP human IgG antibody, was cleaved completely. So the cleavage pattern was not specifically for the CXCR3 antibody.

Therefore the question arose if the used digestion buffer (out of an older $(fab)_2$ was not adequate). However, the same result was demonstrated with a self-made 20mM sodium acetate buffer pH 4,47. The enzyme seemed to have a too high activity. Therefore to slow down the enzyme's activity, less enzyme was used, different temperatures (37°C and room temperature), various incubation times and a higher pH (4,5/5/5,5) were used. The purification step was eliminated after the first attempt because of saving antibody.

The best digest could be achieved in the 20mM sodium acetate buffer (pH 5) at 37°C. It cleaves the antibody into 5 fragments with a size of 100kDa, 75kDa, 55kDa, 25kDa and 10 kDa shown on a non- reducing SDS page (Figure 20). Row number 1 was the standard protein marker and the next three rows were showing the undigested CXCR3 antibody (150 kDa), $(fab)_2$ fragments (110kDa) and a control fab fragment (50 kDa).

It is known that pepsin does cleave the residues of C-Terminus of Phe, Leu, Tyr, Trp, but does not cleave at the amino residues of Alanine, Valine and Glycine residues. [82] Unfortunately, the crystal structure of the CXCR3 is not known and therefore the restriction sites of pepsin might be all over the antibody and not specifically under the hinge region.

Moreover, it was still questionable if the 100kDa fragments were real $(fab)_2$ fragments because they were 20 kDa smaller as the human $(fab)_2$ positive control. However, if the 100kDa were assumed as the desired $(fab)_2$ fragments (because of fewer glycosylation patterns in comparison to a human antibody), two additional purification steps would be necessary (Protein A or G and size exclusion chromatography) to separate the fragments from the other. The yield would be too low to be able to use in an *in- vivo* experiment.

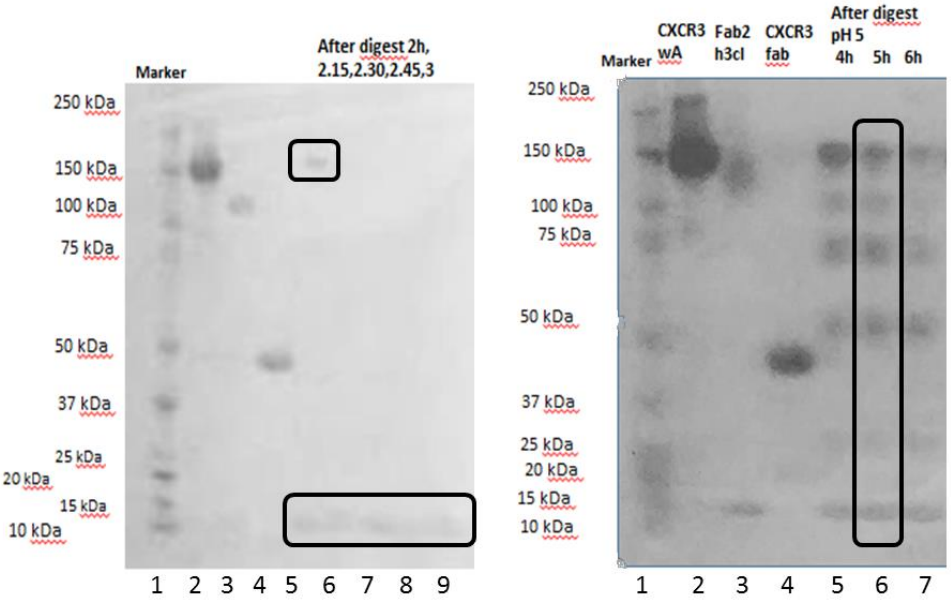

Figure 20: Non-reduced SDS PAGE of pepsin digests

Left: and right row 1: Protein size marker (10-250kDa), row 2: CXCR3 antibody (150kDa), row 3: human $(fab)_2$ control Fragment (110kDa), row 4: CXCR3 fab fragment (48 kDa)

Left:: Row 5-9: Digestion of CXCR3 antibody after an incubation time of 2.15h (150kDa and 10kDa), 2.30h (10kDa), 2.45h (10kDa) and 3h (10kDa)- shown in black framed windows

Right: Row 5-7: Digestion of CXCR3 antibody after an incubation time of 4h, 5h (black frame), 6h in 20mM sodium acetate buffer (pH 5,0) (150 kDa: undigested CXCR3 antibody; 100kDa: might be a non-heavily glycosylated $(Fab)_2$ fragment, 70 kDa,/60kDa/25kDa/10kDa: unspecific cleaved fragments

Taken together, the pepsin digestion seemed to be not the ideal proteolytic enzyme to cleave the Armenian hamster IgG1 CXCR3 antibody.

4.3.2 Ficin

It is already known that specific antibodies, mainly IgG with the subclass 1 are relatively challenging to cleave with pepsin, however, the proteolytic enzyme ficin that is known to cleave reliably mouse IgG1. Based on the immunogenicity of hamster antibody in mice, the new approach was based on a ficin digestion.

SDS PAGE

The SDS PAGE of the ficin digest was displayed in figure 21. It could be demonstrated that the digestion of suggested 24h did not show any cleavage (Figure 21). The evidence was seen in the Protein G column purification (supposing hamster antibodies bind better to Protein G than protein A), where no $(fab)_2$ fragments could be detected in the flow through fraction and the elution only contained undigested antibody, which proves that the digestion did not work. In the second attempt the incubation time was extended to 26h, 26h, 30h and 32h (Figure 21), where aliquots were taken out of the digestion tube.

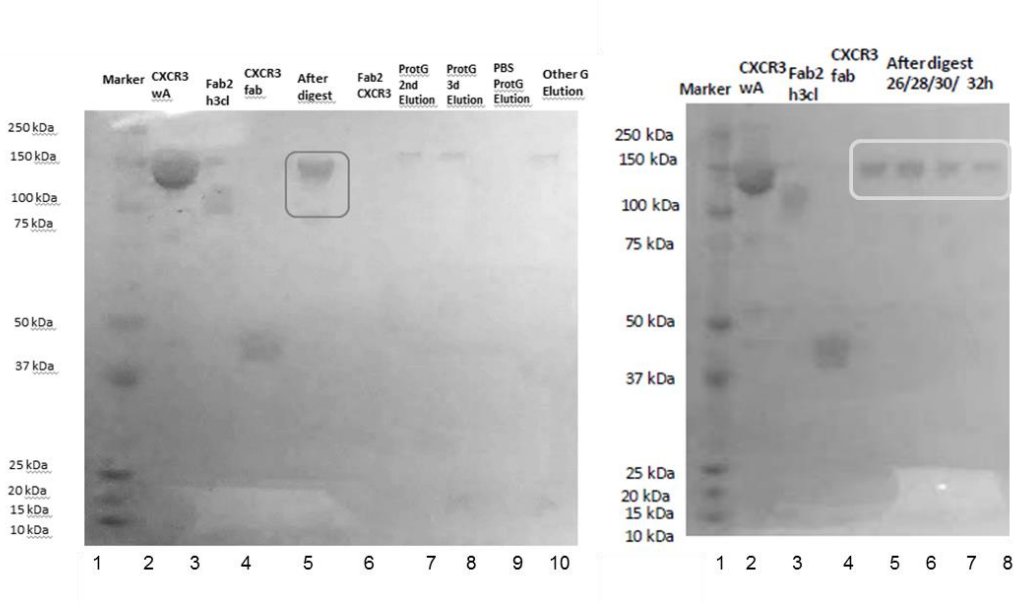

Figure 21: Non-reduced SDS PAGE of ficin digest

Left and right: row 1: Protein size marker (10-250kDa), row 2: CXCR3 antibody (150kDa), row 3: human $(fab)_2$ control Fragment (110kDa), row 4: CXCR3 fab fragment (48 kDa)

Left: row 5: digest with ficin for 24 h (150kDa undigested CXCR3 antibody) (grey framed window), row 6: flow through of Protein G column (none), row 7-10: elution fractions from Protein column G (150kDa: undigested antibody)

Right: row 5-8: digest with ficin for 26h, 28h, 30h and 32h

4.3.3 Papain

Due to the fact that the $(fab)_2$ digestion was surprisingly not possible, the new approach was to cleave the CXCR3 antibody into fab fragments with papain and testing the fragments for their functional properties (binding capacity).

a. SDS PAGE

The papain digestion showed that the CXCR3 antibody could be fragmented into fab fragments, which are illustrated in the reduced SDS PAGE analysis in Figure 22.

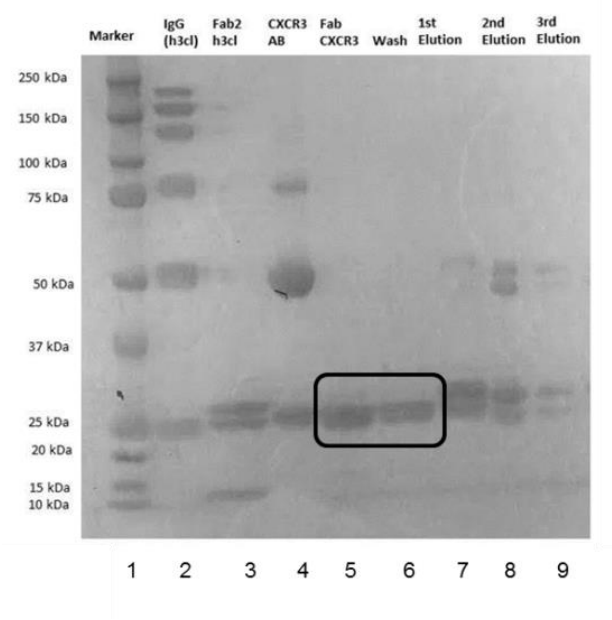

Figure 22: Reduced SDS PAGE of the papain digest

Row 1: Protein size marker (10-250kDa), row 2: human IgG antibody (250kDa, 200kDa, 130 kDa: aggregates and not completely reduced antibody), row 3: human $(fab)_2$ control (25,26 kDa: light and heavy chain of fab2 fragments), row 4: CXCR3 antibody (150kDa), row 5: Flow through CXCR3 fab fragment (25 kDa) after protein A purification, row 6: flow through 2 that contains desired CXCR3 fab fragment (25kDa), row 7: 1^{st} elution of Protein column (26kDa fab fragments, 30kDa Fc parts), row 8: 2^{nd} elution of Protein A column (48/50kDa heavy chain of undigested antibody, 26kDa fab fragments of undigested antibody, 30kDa Fc fragments), row 9: 3^{rd} elution of Protein A (48/50kDa heavy chain of undigested antibody, 26kDa fab fragments of undigested antibody, 30kDa Fc fragments)

Row 1 shows the Protein size marker and rows 2-4 are showing the controls such as an IgG antibody, $(fab)_2$ fragments (no control fab fragment was available at that moment) and the undigested CXCR3 antibody. The whole IgG antibodies were made of two identical heavy chains (50 kDa) and two identical light chains (25 kDa).

Therefore in this reduced SDS gel where β- mercaptoethanol reduced all disulfide bonds, the bands for the desired fab fragment with two light chains appeared at a molecular weight of 25/26kDa (Row 5 and 6 were the digested and purified antibody). Whereas the cleaved long heavy chain was visible at 50 kDa, that could be seen in the control rows 2 and 4 and in the Protein A purification elution fractions 2 and 3 (Row: 8 and 9).

The split-off Fc part was visible in all elution fractions of the protein A purification in row 7, 8 and 9 where the characteristic band appears at 30 kDa. The second elution contains the undigested CXCR3 antibody additionally at 25kDa and 50kDa.

In this case Protein A column was used because it was delivered in the kit and therefore loading buffer and elution buffer were already explicitly optimized for this column.

Based on the Nanodrop measurements it was possible to tell that the total amount of CXCR3 antibody of 3,65 mg is digested into 1,267 mg (35,9%) fab fragments and 2,26 mg (64,1%) of undesired undigested antibody and cleaved Fc parts. The regeneration of total protein after desalting column, digestion and Protein A column is almost 96,9%, that suggests that hardly any protein was lost within the single steps.

b. Analysis of binding capacity by flow cytometry analysis

After generation of the purified papain, the cleaved fab fragments were tested for their binding capacity in a functional *in-vitro* assay and a following flow analysis.

The antibody that was used for incubation and the APC conjugated anti-mouse CXCR3 AB is from the same clone (CXCR3 173), which showed if the unconjugated antibody or fab fragment block the binding site. Therefore the higher the signal, the less binding was expected. The incubation with the fab fragment had less binding capacity in comparison to the whole undigested CXCR3 antibody.

Cytotoxic CD8+ CXCR3+ T cells were analyzed with FlowJo software and were gated on lymphocytes via forward scatter/side scatter, separated into single cells and further gated on CD3+,CD8+,CXCR3+ with the exclusion of B cells (CD19+) and CD4+ T cells.

Figure **23** illustrates the different population sizes of CD8+/CXCR3+ which were untreated, incubated with fab or with the whole antibody (wA). The untreated showed that a cell CXCR3+ and CD8+ cell population was present, whereas the whole antibody eliminated the signal. The fab fragment could only reduce the signal by 17%, whereas the undigested whole antibody showed a 71% decrease of the mean fluorescent intensity signal in comparison to the untreated signal (Figure 24).

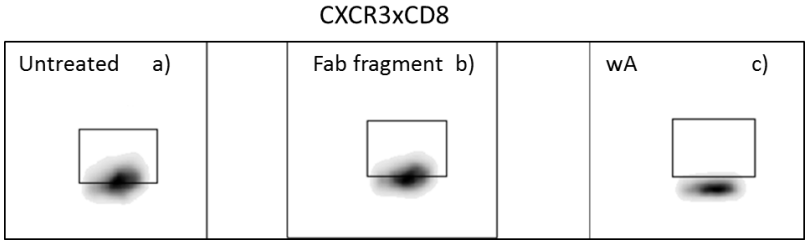

Figure 23: Comparison of CXCR3+ populations treated with none, fab and undigestedCXCR3 antibody
The CD8+ cell population was identified by the markers CD3+/CD8+ which is indicated in the headline of the framed pictures. (X axis vs. Y axis).
a) Untreated, b) fab fragment and c) CXCR3 antibody incubated with CD8+CXCR3+ liver lymphocytes populations

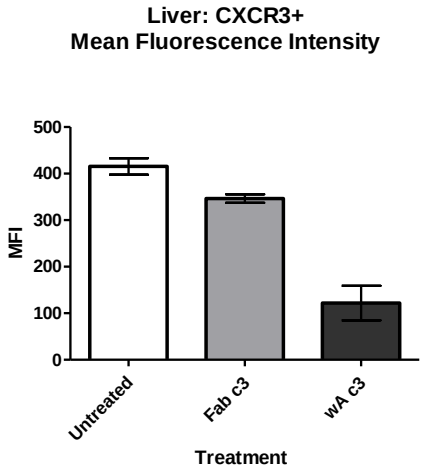

Figure 24: Binding capacity of fab fragment (MFI)

X-axis shows the treatment of the isolated lymphocytes (untreated, fab, wA= undigested CXCR3 antibody)

Y-axis: MFI of CD3+/CD8+/CXCR3+ cells

The graph was made with Graph Pad Prism (Version 5) and statistical significance was excluded due to sample size (only 2 mice).

Conclusively, due to the limitation of the CXCR3 antibody amount, the fab fragments could not be further tested.

5 Discussion and Perspectives

The purpose of the master thesis was to determine if the CXCR3 chemokine receptor is critical to the immune response generated after GAP immunization. First of all, two multicolor flow cytometry panels were developed to identify CXCR3 expressing cells in the livers of immunized mice. At an early time point after infection the detection of CXCR3 expressing CD4+ T cell, CD8+ T cells, NK (T) cells, B cells and plasmacytoid dendritic cells (pDCs) was possible. Moreover, the second flow panel could be illustrated that after six weeks post immunization and a challenge, a high proportion of CXCR3+ expressing antigen-experienced CD8+ memory T cells in the livers was determined, but not in the spleen.
Interestingly, the combination of CXCR3 expression on resident memory CD8+ T and the surface markers (CXCR6 and CD69) have been seen to be crucial for protection after RAS immunization [58] and therefore it might be possible to postulate that these CXCR3 expressing Trm cells are also critical for GAP mediated protection.

This could be shown in the first experiment, where the CXCR3+ cells in immunized C57BL/6 mice were depleted with an anti- CXCR3 antibody, to prove that a CXCR3 expressing cell (CD8+ T cells, Trm cells) are crucial for protection. It could be clearly demonstrated that the loss of the CXCR3 expressing cells led to a high liver burden in the immunized mice, which implies that the protection was lost.
After that result, the second experiment in the CXCR3 knockout mice was set up to see if the CXCR3 receptor is involved in the process. Surprisingly, the immunized CXCR3 knockout mice were sterile protected. There can be multiple reasons for that, first of all, the three immunizations might have already established a robust protective CD8+ memory T cell population in the liver even in the absence of CXCR3. Therefore, in future experiments, it will be necessary to examine if the present cell populations and in particular, the Trm cells are present in the immunized CXCR3 knockout mice at the same levels as in the immunized mice. This can be investigated with the secondly developed Trm cell flow panel.

Moreover, it is possible that CXCR3 only plays a minor role in the Trm cells' recruitment and establishment. Therefore for future experiments, a suboptimal vaccination strategy can be chosen. Unpublished internal laboratory data indicated that only two times vaccinated mice show more likely small differences in protection and thus it enables the opportunity to see if the CXCR3 has a minor impact on mediated protection. Alternatively, the challenge with wildtype GFPLuc sporozoites is injected two months to three months after the last FabB/F immunization to show that CXCR3 is involved in the maintenance of the protective liver Trm cells.
The second reason why the immunized CXCR3 knockout mice still showed protection could be that compensative mechanisms were turned on for the loss of the CXCR3 receptor.

The impact of the innate immune response was also examined. Here, the IVIS analysis showed that the FabB/F injected CXCR3 knockout mice were able to control a secondary liver burden three days post infection. The following flow analysis of CXCR3+ cells confirmed the outcome because no difference in the recruitment of NKT cells to the liver could be detected, which are critical for the innate immune control to pre-erythrocytic malaria infection. [10]
Interestingly, the flow analysis showed that the recruitment of the CD8 + T cells was significantly decreased in the livers of the $CXCR3^{-/-}$ mice. This observation makes it even more surprising that the three times immunized CXCR3 mice in the protection experiment did not show a phenotype. However, the flow panel could only show total CD8+ T cell, but no more precise characterization of the cell populations was possible, due to the lack of specific markers in the flow panel. Therefore a future experiment has to show the phenotype of the activation status CD8+T cell at that time point.
Moreover, it is necessary to phenotype secondary lymph organs (SLOs), such as spleen and lymph nodes [83] at that early time point, to find out if the CD8+ T cells which later might become a liver Trm cells to convey protection. They might be just activated in the SLO and home back to the liver at a later time point. This would also explain why the immunized CXCR3 knockout mice did not show a loss in protection, even though the liver of the CXCR3 knockout mice did show a low number of recruited CD8+ T cells in the innate experiment.

However, the foundation these future hypotheses is that the cell populations of CD8+ T cells are characterized in detail after the innate and the adaptive control experiment to get a step closer to determine the mechanisms.

To eliminate any differences in the genetic background and to be able to address all time points during immunization, a CXCR3 blocking antibody (fragment) was developed. Unfortunately, the digest with the proteolytic enzymes pepsin and ficin could not generate a $(fab)_2$ fragments out of the CXCR3 cell-depleting Armenian hamster antibody. The $(fab)_2$ fragment would advantageous in comparison to fab fragments through extended clearance time and functional properties. The difficulties arose due to the isotype IgG1 of the CXCR3 antibody, which is known to be problematic to cleave. [84] However, in the end, only papain was able to cleave the CXCR3 antibody into fab fragments. They were tested with a flow cytometry-based binding assay which showed that the fab fragment blocked the receptor less efficient as the undigested antibody. Therefore other analysis methods, such as a functional chemotaxis assay [80] or an *in vivo* experiment should be conducted to see if the fab fragment would be a possible candidate for blocking the CXCR3 receptor in mice. An alternative approach to generate a CXCR3 blocking antibody would be the digest with the deglycosylation enzyme PNGaseF that is proposed to diminish the depleting properties of the CXCR3 antibody *in vivo* [85] or to create a polyclonal CXCR3 antibody (fragments) out of rabbits. [86, 87]

Overall, it must be taken into consideration, that the CXCR3 receptor might just not be involved in the control of pre-erythrocytic malaria and other chemokines play a role in the process. As an example, the CXCR6 receptor is critical for the maintenance of Trm cells in the liver after radiated attenuated *P. berghei* sporozoite immunization. [60] The RNAseq analysis of CXCR6 expression showed that it is only under the top 400 most upregulated genes. Therefore the next chosen candidates must be selected with an extended approach through investigating not just the hepatocytes and LSECs RNAseq, but also looking at the upregulated transcripts in activated CD8+ T cells and liver resident memory CD8+ T cells to find out which receptors are expressed at what time point during the immunization process.

In conclusion, the data indicates that CXCR3 is not critical for the recruitment, activation or maintenance of innate immune cells (NKT), but its impact on adaptive immunity needs to be resolved with more detailed experiments. Although CXCR3 might play a role in Trm cell development, there have to be other pathways initiated to modulate the development of an effective Trm cell-mediated protective response. The understanding of how this response is generated is critical to devising ways to both improve GAP vaccine efficacy, but will also be useful for generating approaches to enhance immunity against other liver pathologies.

References

[1] World Health Organization, “World malaria report 2017,”.

[2] A. S. I. Aly, S. A. Mikolajczak, H. S. Rivera et al., “Targeted deletion of SAP1 abolishes the expression of infectivity factors necessary for successful malaria parasite liver infection,” *Molecular microbiology*, vol. 69, no. 1, pp. 152–163, 2008.

[3] N. S. Butler, A. M. Vaughan, J. T. Harty et al., “Whole parasite vaccination approaches for prevention of malaria infection,” *Trends in immunology*, vol. 33, no. 5, pp. 247–254, 2012.

[4] G. J. Keitany, B. Sack, H. Smithers et al., “Immunization of Mice with Live-Attenuated Late Liver Stage-Arresting Plasmodium yoelii Parasites Generates Protective Antibody Responses to Preerythrocytic Stages of Malaria,” *Infection and Immunity*, vol. 82, no. 12, pp. 5143–5153, 2014.

[5] R. S. Klein, E. Lin, B. Zhang et al., “Neuronal CXCL10 Directs CD8+ T-Cell Recruitment and Control of West Nile Virus Encephalitis,” *Journal of virology*, vol. 79, no. 17, pp. 11457–11466, 2005.

[6] I. A. Khan, J. A. MacLean, F. S. Lee et al., “IP-10 is critical for effector T cell trafficking and host survival in Toxoplasma gondii infection,” *Immunity*, vol. 12, no. 5, pp. 483–494, 2000.

[7] U. Christen, D. B. McGavern, A. D. Luster et al., “Among CXCR3 chemokines, IFN-gamma-inducible protein of 10 kDa (CXC chemokine ligand (CXCL) 10) but not monokine induced by IFN-gamma (CXCL9) imprints a pattern for the subsequent development of autoimmune disease,” *Journal of immunology (Baltimore, Md. : 1950)*, vol. 171, no. 12, pp. 6838–6845, 2003.

[8] H. Yoneyama, S. Narumi, Y. Zhang et al., “Pivotal role of dendritic cell-derived CXCL10 in the retention of T helper cell 1 lymphocytes in secondary lymph nodes,” *The Journal of Experimental Medicine*, vol. 195, no. 10, pp. 1257–1266, 2002.

[9] J. H. Dufour, M. Dziejman, M. T. Liu et al., “IFN-gamma-inducible protein 10 (IP-10; CXCL10)-deficient mice reveal a role for IP-10 in effector T cell generation and trafficking,” *Journal of immunology (Baltimore, Md. : 1950)*, vol. 168, no. 7, pp. 3195–3204, 2002.

[10] J. L. Miller, B. K. Sack, M. Baldwin et al., “Interferon-mediated innate immune responses against malaria parasite liver stages,” *Cell reports*, vol. 7, no. 2, pp. 436–447, 2014.

[11] A. S. Tarun, R. F. Dumpit, N. Camargo et al., “Protracted Sterile Protection with Plasmodium yoelii Pre-erythrocytic Genetically Attenuated Parasite Malaria Vaccines Is Independent of Significant Liver-Stage Persistence and Is Mediated by CD8+ T Cells,” *The Journal of Infectious Diseases*, vol. 196, no. 4, pp. 608–616, 2007.

[12] T. C. Luke and S. L. Hoffman, “Rationale and plans for developing a non-replicating, metabolically active, radiation-attenuated Plasmodium falciparum sporozoite vaccine,” *The Journal of experimental biology*, vol. 206, Pt 21, pp. 3803–3808, 2003.

[13] A. S. Tarun, K. Baer, R. F. Dumpit et al., “Quantitative isolation and in vivo imaging of malaria parasite liver stages,” *International journal for parasitology*, vol. 36, no. 12, pp. 1283–1293, 2006.

[14] T. W. A. Kooij, J. M. Carlton, S. L. Bidwell et al., “A Plasmodium whole-genome synteny map: indels and synteny breakpoints as foci for species-specific genes,” *PLoS pathogens*, vol. 1, no. 4, e44, 2005.

[15] D. L. Medica and P. Sinnis, “Quantitative dynamics of Plasmodium yoelii sporozoite transmission by infected anopheline mosquitoes,” *Infection and immunity*, vol. 73, no. 7, pp. 4363–4369, 2005.

[16] R. Amino, S. Thiberge, B. Martin et al., “Quantitative imaging of Plasmodium transmission from mosquito to mammal,” *Nature Medicine*, vol. 12, no. 2, pp. 220–224, 2006.

[17] M. M. Mota, G. Pradel, J. P. Vanderberg et al., “Migration of Plasmodium sporozoites through cells before infection,” *Science (New York, N.Y.)*, vol. 291, no. 5501, pp. 141–144, 2001.

[18] P. S. Gomes, J. Bhardwaj, J. Rivera-Correa et al., “Immune Escape Strategies of Malaria Parasites,” *Frontiers in microbiology*, vol. 7, p. 1617, 2016.

[19] I. Ejigiri and P. Sinnis, “Plasmodium sporozoite-host interactions from the dermis to the hepatocyte,” *Current opinion in microbiology*, vol. 12, no. 4, pp. 401–407, 2009.

[20] S. E. Lindner, J. L. Miller, and S. H. I. Kappe, “Malaria parasite pre-erythrocytic infection: Preparation meets opportunity,” *Cellular microbiology*, vol. 14, no. 3, pp. 316–324, 2012.

[21] N. Bano, J. D. Romano, B. Jayabalasingham et al., “Cellular interactions of Plasmodium liver stage with its host mammalian cell,” *International journal for parasitology*, vol. 37, no. 12, pp. 1329–1341, 2007.

[22] A. M. Vaughan, S. A. Mikolajczak, E. M. Wilson et al., “Complete Plasmodium falciparum liver-stage development in liver-chimeric mice,” *The Journal of clinical investigation*, vol. 122, no. 10, pp. 3618–3628, 2012.

[23] L. H. Miller, D. I. Baruch, K. Marsh et al., “The pathogenic basis of malaria,” *Nature*, vol. 415, 673 EP -, 2002.

[24] J. L. Miller, S. Murray, A. M. Vaughan et al., “Quantitative bioluminescent imaging of pre-erythrocytic malaria parasite infection using luciferase-expressing Plasmodium yoelii,” *PloS one*, vol. 8, no. 4, e60820, 2013.

[25] C. Q Schmidt, A. Kennedy, and W.-H. Tham, “More than just immune evasion: Hijacking complement by Plasmodium falciparum,” vol. 67, 2015.

[26] L. D. Kori, N. Valecha, and A. R. Anvikar, “Insights into the early liver stage biology of Plasmodium,” *Journal of Vector Borne Diseases*, vol. 55, no. 1, p. 9, 2018.

[27] F. Heymann, J. Peusquens, I. Ludwig-Portugall et al., “Liver inflammation abrogates immunological tolerance induced by Kupffer cells,” *Hepatology (Baltimore, Md.)*, vol. 62, no. 1, pp. 279–291, 2015.

[28] S. T. Agnandji, B. Lell, J. F. Fernandes et al., “A phase 3 trial of RTS,S/AS01 malaria vaccine in African infants,” *The New England journal of medicine*, vol. 367, no. 24, pp. 2284–2295, 2012.

[29] J. C. Pringle, G. Carpi, J. Almagro-Garcia et al., “RTS,S/AS01 malaria vaccine mismatch observed among Plasmodium falciparum isolates from southern and central Africa and globally,” *Scientific reports*, vol. 8, no. 1, p. 6622.

[30] E. M. Bijker, G. J. H. Bastiaens, A. C. Teirlinck et al., “Protection against malaria after immunization by chloroquine prophylaxis and sporozoites is mediated by preerythrocytic immunity,” *Proceedings of the National Academy of Sciences of the United States of America*, vol. 110, no. 19, pp. 7862–7867, 2013.

[31] D. I. Stanisic, J. S. McCarthy, and M. F. Good, “Controlled Human Malaria Infection: Applications, Advances, and Challenges,” *Infection and immunity*, vol. 86, no. 1, 2018.

[32] A. S Ishizuka, K. Lyke, A. DeZure et al., “Protection against malaria at 1 year and immune correlates following PfSPZ vaccination,” vol. 22, 2016.

[33] D. F. Clyde, V. C. McCarthy, R. M. Miller et al., “Specificity of protection of man immunized against sporozoite-induced falciparum malaria,” *The American journal of the medical sciences*, vol. 266, no. 6, pp. 398–403, 1973.

[34] W. E. Collins and P. G. Contacos, “Immunization of monkeys against Plasmodium cynomolgi by X-irradiated sporozoites,” *Nature: New biology*, vol. 236, no. 67, pp. 176–177, 1972.

[35] R. S. Nussenzweig, J. Vanderberg, H. Most et al., “Protective immunity produced by the injection of x-irradiated sporozoites of plasmodium berghei,” *Nature*, vol. 216, no. 5111, pp. 160–162, 1967.

[36] R. Ménard and C. Janse, “Gene targeting in malaria parasites,” *Methods (San Diego, Calif.)*, vol. 13, no. 2, pp. 148–157, 1997.

[37] A. M. Vaughan, M. T. O'Neill, A. S. Tarun et al., “Type II fatty acid synthesis is essential only for malaria parasite late liver stage development,” *Cellular microbiology*, vol. 11, no. 3, pp. 506–520, 2009.

[38] A. Trimnell, A. Takagi, M. Gupta et al., “Genetically attenuated parasite vaccines induce contact-dependent CD8+ T cell killing of Plasmodium yoelii liver stage-infected hepatocytes,” *Journal of immunology (Baltimore, Md. : 1950)*, vol. 183, no. 9, pp. 5870–5878, 2009.

[39] N. S. Butler, N. W. Schmidt, A. M. Vaughan et al., “Superior antimalarial immunity after vaccination with late liver stage-arresting genetically attenuated parasites,” *Cell host & microbe*, vol. 9, no. 6, pp. 451–462, 2011.

[40] P. Liehl and M. M. Mota, “Innate recognition of malarial parasites by mammalian hosts,” *International journal for parasitology*, vol. 42, no. 6, pp. 557–566, 2012.

[41] P. Liehl, P. Meireles, I. S. Albuquerque et al., “Innate immunity induced by Plasmodium liver infection inhibits malaria reinfections,” *Infection and immunity*, vol. 83, no. 3, pp. 1172–1180, 2015.

[42] J. R. Groom and A. D. Luster, “CXCR3 ligands: Redundant, collaborative and antagonistic functions,” *Immunology and cell biology*, vol. 89, no. 2, pp. 207–215, 2011.

[43] P. J. Brennan, M. Brigl, and M. B. Brenner, “Invariant natural killer T cells: An innate activation scheme linked to diverse effector functions,” *Nature reviews. Immunology*, vol. 13, no. 2, pp. 101–117, 2013.

[44] P. Sharma, K. Wagner, J. D. Wolchok et al., “Novel cancer immunotherapy agents with survival benefit: Recent successes and next steps,” *Nature Reviews Cancer*, vol. 11, no. 11, p. 805, 2011.

[45] M. B. Drennan, A.-S. Franki, P. Dewint et al., “Cutting edge: the chemokine receptor CXCR3 retains invariant NK T cells in the thymus,” *Journal of immunology (Baltimore, Md. : 1950)*, vol. 183, no. 4, pp. 2213–2216, 2009.

[46] “Innate vs. Adaptive Immunity - Immunology - Medbullets Step 1,” https://step1.medbullets.com/immunology/105041/innate-vs-adaptive-immunity.

[47] K. Kimura, D. Kimura, Y. Matsushima et al., “CD8+ T Cells Specific for a Malaria Cytoplasmic Antigen Form Clusters around Infected Hepatocytes and Are Protective at the Liver Stage of Infection,” *Infection and immunity*, vol. 81, no. 10, pp. 3825–3834, 2013.

[48] M. F. Good and D. L. Doolan, “Malaria vaccine design: immunological considerations,” *Immunity*, vol. 33, no. 4, pp. 555–566, 2010.

[49] J. Ibrahim, A. H. Nguyen, A. Rehman et al., “Dendritic Cell Populations With Different Concentrations of Lipid Regulate Tolerance and Immunity in Mouse and Human Liver,” *Gastroenterology*, vol. 143, no. 4, pp. 1061–1072, 2012.

[50] D. Wohlleber, H. Kashkar, K. Gärtner et al., “TNF-Induced Target Cell Killing by CTL Activated through Cross-Presentation,” *Cell reports*, vol. 2, no. 3, pp. 478–487, 2012.

[51] L. Diehl, A. Schurich, R. Grochtmann et al., “Tolerogenic maturation of liver sinusoidal endothelial cells promotes B7-homolog 1-dependent CD8+ T cell tolerance,” *Hepatology (Baltimore, Md.)*, vol. 47, no. 1, pp. 296–305, 2008.

[52] J. P. Böttcher, O. Schanz, D. Wohlleber et al., “Liver-Primed Memory T Cells Generated under Noninflammatory Conditions Provide Anti-infectious Immunity,” *Cell reports*, vol. 3, no. 3, pp. 779–795, 2013.

[53] A. Le Bon, N. Etchart, C. Rossmann et al., “Cross-priming of $CD8^+$ T cells stimulated by virus-induced type I interferon,” *Nature Immunology*, vol. 4, no. 10, p. 1009, 2003.

[54] N. S. Butler, N. W. Schmidt, and J. T. Harty, “Differential effector pathways regulate memory CD8 T cell immunity against Plasmodium berghei versus P. yoelii sporozoites,” *Journal of immunology (Baltimore, Md. : 1950)*, vol. 184, no. 5, pp. 2528–2538, 2010.

[55] J. Schumann, K. Stanko, U. Schliesser et al., “Differences in CD44 Surface Expression Levels and Function Discriminates IL-17 and IFN-γ Producing Helper T Cells,” *PloS one*, vol. 10, no. 7, e0132479, 2015.

[56] S. M. Kaech and W. Cui, “Transcriptional control of effector and memory CD8+ T cell differentiation,” *Nature reviews. Immunology*, vol. 12, no. 11, pp. 749–761, 2012.

[57] J. M. Schenkel and D. Masopust, “Tissue-resident memory T cells,” *Immunity*, vol. 41, no. 6, pp. 886–897, 2014.

[58] D. Fernandez-Ruiz, W. Y. Ng, L. E. Holz et al., “Liver-Resident Memory CD8+T Cells Form a Front-Line Defense against Malaria Liver-Stage Infection,” *Immunity*, vol. 45, no. 4, pp. 889–902, 2016.

[59] M. G. Overstreet, Y.-C. Chen, I. A. Cockburn et al., “CD4+ T cells modulate expansion and survival but not functional properties of effector and memory CD8+ T cells induced by malaria sporozoites,” *PloS one*, vol. 6, no. 1, e15948, 2011.

[60] N. Iijima and A. Iwasaki, “Tissue instruction for migration and retention of TRM cells,” *Trends in immunology*, vol. 36, no. 9, pp. 556–564, 2015.

[61] F. Stelma, A. de Niet, M. J. Sinnige et al., “Human intrahepatic CD69 + CD8+ T cells have a tissue resident memory T cell phenotype with reduced cytolytic capacity,” *Scientific reports*, vol. 7, no. 1, p. 6172, 2017.

[62] S.-W. Tse, A. J. Radtke, D. A. Espinosa et al., “The chemokine receptor CXCR6 is required for the maintenance of liver memory $CD8^+$ T cells specific for infectious pathogens,” *The Journal of infectious diseases*, vol. 210, no. 9, pp. 1508–1516, 2014.

[63] X. Fan and A. Y. Rudensky, “Hallmarks of Tissue-Resident Lymphocytes,” *Cell*, vol. 164, no. 6, pp. 1198–1211, 2016.

[64] H. A. McNamara, Y. Cai, M. V. Wagle et al., “Up-regulation of LFA-1 allows liver-resident memory T cells to patrol and remain in the hepatic sinusoids,” *Science immunology*, vol. 2, no. 9, 2017.

[65] F. Sallusto, D. Lenig, R. Förster et al., “Two subsets of memory T lymphocytes with distinct homing potentials and effector functions,” *Nature*, vol. 401, no. 6754, p. 708, 1999.

[66] B. V. Kumar, W. Ma, M. Miron et al., “Human Tissue-Resident Memory T Cells Are Defined by Core Transcriptional and Functional Signatures in Lymphoid and Mucosal Sites,” *Cell reports*, vol. 20, no. 12, pp. 2921–2934, 2017.

[67] D. T. Graves and Y. Jiang, “Chemokines, a family of chemotactic cytokines,” *Critical reviews in oral biology and medicine : an official publication of the American Association of Oral Biologists*, vol. 6, no. 2, pp. 109–118, 1995.

[68] E. K. Lau, C. D. Paavola, Z. Johnson et al., “Identification of the glycosaminoglycan binding site of the CC chemokine, MCP-1: implications for structure and function in vivo,” *The Journal of biological chemistry*, vol. 279, no. 21, pp. 22294–22305, 2004.

[69] A. E. I. Proudfoot, T. M. Handel, Z. Johnson et al., “Glycosaminoglycan binding and oligomerization are essential for the in vivo activity of certain chemokines,” *Proceedings of the National Academy of Sciences of the United States of America*, vol. 100, no. 4, pp. 1885–1890, 2003.

[70] D. C. T. Palomino and L. C. Marti, “Chemokines and immunity,” *Einstein*, vol. 13, no. 3, pp. 469–473, 2015.

[71] Q. Wang, D. R. Nagarkar, E. R. Bowman et al., “Role of double-stranded RNA pattern recognition receptors in rhinovirus-induced airway epithelial cell responses,” *Journal of immunology (Baltimore, Md. : 1950)*, vol. 183, no. 11, pp. 6989–6997, 2009.

[72] Nuska Tschammer, ed., *Chemokines*: *Chemokines and their receptors in drug discovery*, Springer, Switzerland, 2015.

[73] Y. Zohar, G. Wildbaum, R. Novak et al., “CXCL11-dependent induction of FOXP3-negative regulatory T cells suppresses autoimmune encephalomyelitis,” *The Journal of clinical investigation*, vol. 124, no. 5, pp. 2009–2022, 2014.

[74] D. T. Groves and Y. Jiang, “Chemokines, a Family of Chemotactic Cytokines,” *Critical Reviews in Oral Biology & Medicine*, vol. 6, no. 2, pp. 109–118, 1995.

[75] Y. H. Oo, S. Shetty, and D. H. Adams, “The role of chemokines in the recruitment of lymphocytes to the liver,” *Digestive diseases (Basel, Switzerland)*, vol. 28, no. 1, pp. 31–44, 2010.

[76] A. Viola and A. D. Luster, “Chemokines and their receptors: Drug targets in immunity and inflammation,” *Annual review of pharmacology and toxicology*, vol. 48, pp. 171–197, 2008.

[77] N. Kobayashi, T. Kondo, H. Takata et al., “Functional and phenotypic analysis of human memory CD8+ T cells expressing CXCR3,” *Journal of leukocyte biology*, vol. 80, no. 2, pp. 320–329, 2006.

[78] T. R. Schleicher, J. Yang, M. Freudzon et al., “A mosquito salivary gland protein partially inhibits Plasmodium sporozoite cell traversal and transmission,” *Nature Communications*, vol. 9, no. 1, p. 2908.

[79] I. N. Crispe, “Isolation of mouse intrahepatic lymphocytes,” *Current protocols in immunology*, Chapter 3, Unit 3.21, 2001.

[80] R. Uppaluri, K. C. F. Sheehan, L. Wang et al., “Prolongation of cardiac and islet allograft survival by a blocking hamster anti-mouse CXCR3 monoclonal antibody,” *Transplantation*, vol. 86, no. 1, pp. 137–147, 2008.

[81] P. X. Liew, J. H. Kim, W.-Y. Lee et al., “Antibody-dependent fragmentation is a newly identified mechanism of cell killing in vivo,” *Scientific reports*, vol. 7, no. 1, p. 10515, 2017.

[82] D. W. Piper and B. H. Fenton, “pH stability and activity curves of pepsin with special reference to their clinical importance,” *Gut*, vol. 6, no. 5, pp. 506–508, 1965.

[83] A. J. Radtke, S.-W. Tse, and F. Zavala, “From the draining lymph node to the liver: the induction and effector mechanisms of malaria-specific CD8+ T cells,” *Seminars in immunopathology*, vol. 37, no. 3, pp. 211–220, 2015.

[84] C.-G. Liu, M.-C. Zhu, and Z.-N. Chen, “Preparation and purification of F(ab’)2 fragment from anti hepatoma mouse IgG1 mAb,” *World Journal of Gastroenterology*, vol. 5, no. 6, pp. 522–524, 1999.

[85] L. Liu, “Antibody glycosylation and its impact on the pharmacokinetics and pharmacodynamics of monoclonal antibodies and Fc-fusion proteins,” *Journal of pharmaceutical sciences*, vol. 104, no. 6, pp. 1866–1884, 2015.

[86] S. He, Q. Cao, Y. Qiu et al., “A New Approach to the Blocking of Alloreactive T Cell-Mediated Graft-versus-Host Disease by In Vivo Administration of Anti-CXCR3 Neutralizing Antibody,” *The Journal of Immunology*, vol. 181, no. 11, pp. 7581–7592, 2008.

[87] J. H. Xie, N. Nomura, M. Lu et al., “Antibody-mediated blockade of the CXCR3 chemokine receptor results in diminished recruitment of T helper 1 cells into sites of inflammation,” *Journal of leukocyte biology*, vol. 73, no. 6, pp. 771–780, 2003.

List of figures

List of tables

Index of Abbreviation

GAP	Genetically attenuated *Plasmodium*
Py	*Plasmodium yoelii*
LAGAP	Late arresting genetically attenuated *Plasmodium*
WT	wildtype
RBC	Red blood cells
PBS	Phosphate buffered saline

Appendices

Appendix 1: CXCL9 and CXCL10 transcripts are highly upregulated in hepatocytes isolated from *Py* GAP (FabBF-) infected mice

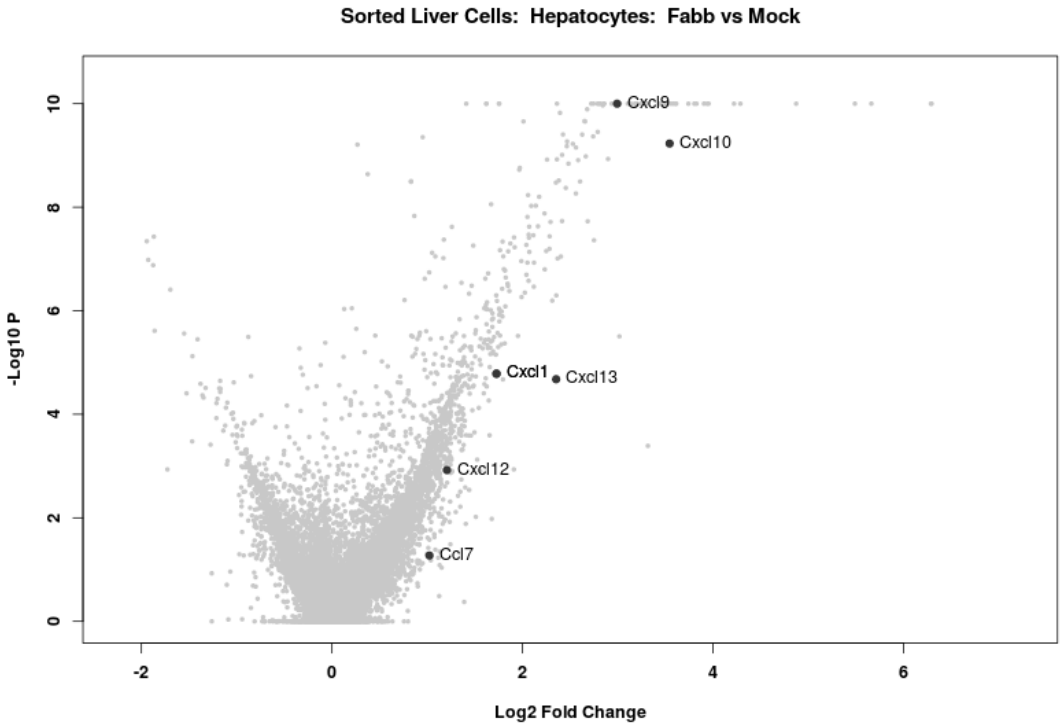

Volcano plot; Comparative RNASeq analysis. Normalized transcript abundances are depicted along with log2 Ratio (FabB/F/ mock), p value, gene description, and chromosomal location of expressed genes. Only transcripts with p values of less than 0.01 and at least 4-fold difference in expression (i.e., log fold > 2) were considered significant.

Appendix 2: CXCL9 and CXCL10 transcripts are highly upregulated in LSECs isolated from *Py* GAP (FabBF-) infected mice

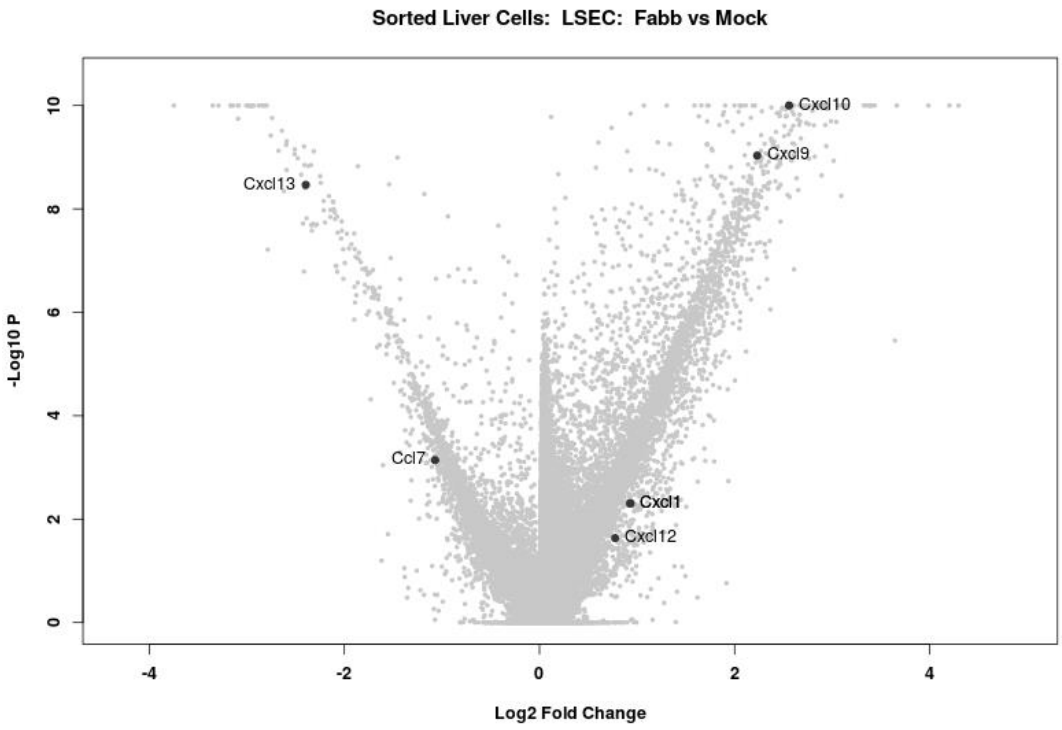

Volcano plot; Comparative RNASeq analysis. Normalized transcript abundances are depicted along with log2 Ratio (FabB/F/ mock), p value, gene description, and chromosomal location of expressed genes. Only transcripts with p values of less than 0.01 and at least 4-fold difference in expression (i.e., log fold > 2) were considered significant.

Appendix 3: Flow cytometer configurations

LSRII Rainier		LSRII Baker		Aria		PMT	Fluorochromes Listed on Configurations
407 nm Laser		405 nm Laser		405 nm Laser			
	450/50		450/50		450/50	H	Pac Blue; Amine Violet; Live Dead Violet
535 LP	550/40	495 LP	525/50	544 LP	545/30	G	Pac Orange
557 LP	560/40	535 LP	550/40	555 LP	560/40	F	Qdot 565
570 LP	585/42	555 LP	586/15	570 LP	585/42	E	Qdot 585
595 LP	605/40	595 LP	610/20	595 LP	605/40	D	Qdot 605
640 LP	660/40	630 LP	670/30	630 LP	660/20	C	Qdot 655
670 LP	705/70	685 LP	710/50	670 LP	705/70	B	Qdot 705
740 LP	780/60	735 LP	780/60	740 LP	780/60	A	Qdot 800
488 nm Laser		488 nm Laser		488 nm Laser			
	488/10		488/10		488/10	C	SSC
505 LP	515/20	505 LP	525/50	505 LP	515/20	B	FITC; AlexFluor 488; GFP; CFSE
685 LP	710/50	685 LP	710/50	685 LP	710/50	A	PerCP-Cy5-5
532 nm Laser		532 nm Laser		532 nm Laser			
	575/25		575/26		575/25	E	PE; EtBr
600 LP	610/20	600 LP	610/20	600 LP	610/20	D	PE-Texas Red
640 LP	660/40	635 LP	670/30	635 LP	660/40	C	PE-Cy5; PerCP; 7AAD
690 LP	710/50	685 LP	710/50	685 LP	710/50	B	PE-Cy5-5
740 LP	780/60	735 LP	780/60	750 LP	780/60	A	PE-Cy7
633 nm Laser		633 nm Laser		640 nm Laser			
	660/20		670/30		660/20	C	APC; AlexaFluor 647
685 LP	710/50	685 LP	730/45	685 LP	730/45	B	APC-Cy55; AlexaFluor 700
740 LP	780/60	735 LP	780/60	740 LP	780/60	A	APC-Cy7

Appendix 4: CXCR3 expressing cells

CD8+ CD44+/CD62L-/ CXCR3+

Spleen naive	Spleen infected	Liver naive	Liver immunized
1.25	6.9	36.70	67.8

CD4+ CD44+/CD62L-/ CXCR3+

Spleen naive	Spleen infected	Liver naive	Liver immunized
8.72	21.5	79.10	88.1

Appendix 5: CXCR3+ Trms located in liver

Total counts

Spleen naive	Spleen infected	Liver naive	Liver immunized
6.	545.	1931.	26880.

Appendix 6: IVIS data of protection experiment (CXCR3 antibody treatment)

Total flux (p/s)

Mock and igG	FabB/F+ IgG	Mock + CXCR3	FabB/F+ CXCR3
465000.00	61800.00	508000.00	104000.00
593000.00	62500.00	846000.00	282000.00
1340000.00	60600.00	246000.00	168000.00
3590000.00	55800.00	151000.00	425000.00
		846000.00	259000.00

Appendix 7: IVIS data of protection experiment (CXCR3 knockout mice)

Total flux (p/s)

C57BL/6J+ Mock	C57BL/6J+ FabB/F	CXCR3+ Mock	CXCR3 + FabB/F
8200000.00	77300.00	2020000.00	142000.00
4430000.00	174000.00	4020000.00	122000.00
2600000.00	35400.00	1800000.00	204000.00
2470000.00	27200.00	2120000.00	111000.00
3130000.00	57900.00	4490000.00	133000.00

Appendix 8: IVIS data of innate immune response

C57BL/6J + Mock	C57BL/6J+ FabB/F	CXCR3-/- + Mock	CXCR3-/-+FabB/F
1310000.00	31800.00	2950000.00	101000.00
2600000.00	238000.00	58000.00	381000.00
1850000.00	517000.00	1300000.00	48400.00
51900.00		53600.00	1080000.00

Appendix 9: Recruitment Experiment - Flow Analysis

% of cell population out of single cells

% out of single cells	B220+	CD3+	CD4+	CD8+	pDc	NK	NKT	Total Coun
Specimen_003_CXCR3 Mock 1_012.fcs	7.28	52.2	31.1	4.71	5.97	2.81	2.29	3100000
Specimen_003_CXCR3 Mock 2_013.fcs	6.39	51.9	28.5	9.52	4.65	9.59	4.1	1900000
Specimen_003_CXCR3 Mock 3_014.fcs	4.36	51.7	31.8	4.42	9.21	1.88	2.11	5500000
Specimen_003_CXCR3 100K 1_009.fcs	3.72	63.5	36.9	9.04	3.13	5.95	5.13	6700000
Specimen_003_CXCR3 100K 2_010.fcs	4.14	59.2	30.9	12.3	4.11	7.53	5.74	7600000
Specimen_003_CXCR3 100K 3_011.fcs	3.83	52.6	27.9	11.5	2.7	6.11	6.05	4900000
Specimen_003_C57BL6 Mock 1_018.fcs	3.67	55.7	28	14	1.4	5.13	3.22	1100000
Specimen_003_C57BL6 Mock 2_019.fcs	3.77	43.5	20.8	5.85	7	2.58	3.73	2500000
Specimen_003_C57BL6 Mock 3_020.fcs	4.24	50.2	24.2	7.36	4.26	2.91	3.09	1600000
Specimen_003_C57BL6 100K 1_015.fcs	2.86	69.4	29.5	24.5	1.82	4.75	6.8	14600000
Specimen_003_C57BL6 100K 2_016.fcs	3.62	71.2	27.1	30.4	1.43	4.67	7.12	9400000
Specimen_003_C57BL6 100K 3_017.fcs	2.63	68	28	25.7	2.47	3.91	8.78	15000000
Specimen_003_FMO Bst2_026.fcs	3.21%	63.90%	29.50%	19.80%	0 %	5.09%	6.49%	
Specimen_003_FMO CD3_022.fcs	3.25%	0.63%	0.10%	0.31%	2.15%	17.60%	0.32%	
Specimen_003_FMO CD4_023.fcs	3.46%	65.20%	0.01%	20.30%	2.29%	4.96%	6.83%	
Specimen_003_FMO CD8_024.fcs	3.26%	65.70%	29.60%	9.00E-06	2.32%	5.00%	6.91%	
Specimen_003_FMO Dx5_025.fcs	3.24%	61.10%	28.40%	18.20%	2.15%	3.59E-05	0.03%	
Specimen_003_FMO Ly6c_027.fcs	4.71%	64.50%	28.70%	20.10%	0 %	5.09%	5.85%	
Specimen_003_Fmo B220_021.fcs	0.02%	65.00%	29.20%	19.60%	1.36E-05	4.95%	5.45%	

Appendix 10: Fab binding capacity assay: MFI of CXCR3+ cells

	Untreated	Fab (28 µg)	CXCR3 AB (28 µg)
Mouse 1	428	353	148
Mouse 2	403	340	95